



HAL
open science

Multi-Knock-a multi-targeted genome-scale CRISPR toolbox to overcome functional redundancy in plants

Yangjie Hu, Priyanka Patra, Odelia Pisanty, Anat Shafir, Zeinu Mussa Belew, Jenia Binenbaum, Shir Ben Yaakov, Bihai Shi, Laurence Charrier, Gal Hyams, et al.

► To cite this version:

Yangjie Hu, Priyanka Patra, Odelia Pisanty, Anat Shafir, Zeinu Mussa Belew, et al.. Multi-Knock-a multi-targeted genome-scale CRISPR toolbox to overcome functional redundancy in plants. *Nature Plants*, In press, 10.1038/s41477-023-01374-4 . hal-04059773

HAL Id: hal-04059773

<https://cnrs.hal.science/hal-04059773>

Submitted on 5 Apr 2023

HAL is a multi-disciplinary open access archive for the deposit and dissemination of scientific research documents, whether they are published or not. The documents may come from teaching and research institutions in France or abroad, or from public or private research centers.

L'archive ouverte pluridisciplinaire **HAL**, est destinée au dépôt et à la diffusion de documents scientifiques de niveau recherche, publiés ou non, émanant des établissements d'enseignement et de recherche français ou étrangers, des laboratoires publics ou privés.

1 **Multi-Knock – a multi-targeted genome-scale CRISPR toolbox to overcome functional**
2 **redundancy in plants**

3 Yangjie Hu¹, Priyanka Patra^{1,2,*}, Odelia Pisanty^{1,*}, Anat Shafir¹, Zeinu Mussa Belew³, Jenia Binenbaum¹, Shir Ben
4 Yaakov¹, Bihai Shi², Laurence Charrier⁴, Gal Hyams¹, Yuqin Zhang¹, Maor Trabolsky¹, Omer Calderaru¹, Daniela
5 Weiss¹, Christoph Crocoll³, Adi Avni¹, Teva Vernoux², Markus Geisler⁴, Hussam Hassan Nour-Eldin³, Itay
6 Mayrose^{1,✉}, and Eilon Shani^{1,✉}

7
8 ¹ School of Plant Sciences and Food Security, Tel Aviv University, Tel Aviv, 69978, Israel

9 ² Laboratoire Reproduction et Développement des Plantes, Université de Lyon, ENS de Lyon, CNRS, INRAE,
10 Lyon, France

11 ³ DynaMo Center, Department of Plant and Environmental Sciences, University of Copenhagen, Frederiksberg,
12 1871, Denmark

13 ⁴ Department of Biology, University of Fribourg, CH-1700 Fribourg, Switzerland

14 * Equal contribution

15 ✉ Corresponding author

16
17 **Abstract**

18 Plant genomes are characterized by large and complex gene families that often result in similar and partially
19 overlapping functions¹. This genetic redundancy severely hampers current efforts to uncover novel
20 phenotypes, delaying basic genetic research and breeding programs². Here, we describe the development
21 and validation of Multi-Knock, a genome-scale CRISPR toolbox that overcomes functional redundancy in
22 *Arabidopsis* by simultaneously targeting multiple gene-family members, thus identifying genetically
23 hidden components. We computationally designed 59,129 optimal single guide RNAs (sgRNAs) that each target
24 2 to 10 genes within a family at once. Furthermore, partitioning the library into ten sub-libraries directed towards
25 a different functional group allows flexible and targeted genetic screens. From the 5,635 sgRNAs targeting
26 the plant transcriptome, we generated over 3,500 independent *Arabidopsis* lines that allowed us to identify
27 and characterize the first known cytokinin tonoplast-localized transporters in plants. With the ability to
28 overcome functional redundancy in plants at the genome-scale level, the developed strategy can be readily
29 deployed by scientists and breeders for basic research and to expedite breeding efforts.

33 **Introduction**

34 Plant genomics research and breeding programs rely on variation, be it natural, induced, or introduced.
35 Phenotypic variation has been the basis for the identification of novel traits and their introduction into robust
36 elite cultivars. Genetic variation has been expanded over the years by introducing natural variation and by
37 creating random mutagenized lines by treatment with physical (e.g., radiation), chemical (e.g., ethyl
38 methanesulfonate), or biological (e.g., T-DNA insertion or gene silencing) mutagens³⁻⁹. These approaches
39 have greatly facilitated and accelerated progress in plant functional genomics and breeding programs over
40 the past several decades.

41 Comprehensive genetic studies and large-scale genome sequencing projects have shown that it is
42 challenging to uncover many phenotypes due to widespread genetic redundancy in plant genomes. A
43 recurrent history of whole-genome duplications and numerous local duplications of smaller scale over the
44 course of plant evolution has resulted in large gene families of similar sequences and partially overlapping
45 functions. On average, 64.5% of plant genes are part of paralogous gene families, ranging from 45.5% in
46 the moss *Physcomitrella patens* to 84.4% in the apple *Malus domestica*¹. Given that ancient and fast-
47 evolving paralogs are not easily detected due to sequence divergence, these percentages are likely
48 underestimates. In *Arabidopsis* (*Arabidopsis thaliana*), the paralogous gene content, genes belonging to
49 families with at least two members, vary from 63% to 78% depending on the methodological procedures
50 applied^{1,4}. It is speculated that single-copy genes are involved in the maintenance of genome integrity and
51 organelle function, whereas multi-copy genes encode proteins involved in signaling, transport, and
52 metabolism¹⁰. Therefore, in many cases mutating multiple gene family members is required to uncover
53 "hidden" phenotypes associated with gene functions².

54 Approaches creating random mutations for forward-genetics (e.g., alkylating agents and T-DNA lines)
55 cannot overcome the limitations of genetic redundancy by simultaneously targeting multiple homologous
56 genes in a single mutant line^{5,11}. In recent years, significant progress has been made using genome-scale
57 RNA interference methods and artificial microRNA (amiRNA) collections^{4,8,9}. However, these methods do
58 not work well in several important crops and generally reduce gene expression rather than cause complete
59 knockout phenotypes¹².

60 Recently, the CRISPR/Cas9 system (Clustered Regularly Interspaced Short Palindromic Repeats),
61 involving CRISPR repeat-spacer arrays and Cas proteins, has been used to build large knockout mutant
62 libraries for forward-genetic screens and analysis of gene functions and regulation. This system represents
63 a tremendous breakthrough for generating targeted mutations both in terms of simplicity and efficiency^{13,14}.
64 In the past few years, studies have demonstrated the feasibility of CRISPR-based knockout collections in
65 rice (*Oryza sativa* L.), maize (*Zea mays*) and tomato (*Solanum lycopersicum*)^{12,15-22}. However, thus far,

66 CRISPR/Cas9 has not been used on a genome-scale level to simultaneously target multiple potentially
67 redundant genes in plants or other eukaryotes.

68 Here, we describe the development and validation of Multi-Knock, a novel genetic approach in plants that
69 combines forward-genetics with dynamically targeted genome-scale CRISPR/Cas9 tools to address the
70 problem of masked phenotypic variation due to functional redundancy (**Fig. 1**). A total of 59,129 multi-
71 targeted sgRNAs, divided into 10 functional sub-libraries targeting 16,152 genes in *Arabidopsis*, were
72 designed, synthesized, and cloned into a genome-editing intronized Cas9 vector²³. From this collection,
73 5,635 sgRNAs targeting 1,123 of the 1,327 transporters (TRP) in *Arabidopsis* were cloned into four
74 different Cas9 vectors generating independent CRISPR libraries, wherein each sgRNA was designed to
75 target closely related homologues within sub-clades in transporter families. A proof of concept forward-
76 genetic screen using over 3,500 CRISPR lines targeting the plant transportome recovered multiple known
77 phenotypes in *Arabidopsis*, demonstrating the validity of the approach. Moreover, our screen allowed us to
78 uncover novel transporters whose function has been hidden due to genetic redundancy. Specifically, we
79 identified a homologous subfamily of three previously unstudied genes with partially overlapping function,
80 *PUP7*, *PUP21*, and *PUP8*. We discovered that while all three proteins biochemically function as cytokinin
81 transporters, *PUP8* localizes to the plasma membrane, while *PUP7* and *PUP21* are localized to the tonoplast.
82 We show that these proteins regulate meristem size, phyllotaxis, and plant growth, revealing complex
83 redundant activity within this sub-family and providing a demonstration of the power of the Multi-Knock
84 approach to discover new biological functions.

85

86 **Results**

87 **Design of a multi-targeted, CRISPR-based, genome-scale genetic toolbox**

88 The high similarity in coding sequences within plant gene families often results in complete, partial, or
89 conditional functional redundancy, leading to substantial phenotypic buffering. To construct a genome-
90 scale library of sgRNAs that would potentially target multiple members from the same family, all gene
91 families in the *Arabidopsis* genome (TAIR10), encompassing 27,416 protein-coding genes, were
92 downloaded from the PLAZA 3.0 plant comparative genomics database²⁴. Following the filtration of
93 mitochondrial and chloroplast genes, as well as singletons (i.e., genes without any family members), 21,798
94 genes remained, belonging to 3,892 families of size 2 or more. We then designed a set of sgRNAs that
95 would optimally target multiple members of each gene family while accounting for the similarity among
96 family members (**Fig. 2a,b**). Specifically, a phylogenetic reconstruction strategy was used to hierarchically
97 organize each family into a tree structure, such that a homologous subgroup of genes that are more closely
98 related are placed closer to each other on the tree. The optimal sgRNAs that could most efficiently target

99 multiple members of each subgroup were designed using the CRISPyS algorithm²⁵. Since CRISPyS could
100 potentially design the same sgRNAs for different subgroups of the same family, we considered only one
101 occurrence of each sgRNA (**Fig. 2c,d**). This procedure resulted in a total of 2,183,722 sgRNAs. Next, we
102 removed sgRNAs that targeted only a single gene with high efficiency, resulting in 1,101,799 sgRNAs. We
103 then removed sgRNAs with potential high off-target activity towards unintended *Arabidopsis* coding
104 regions and filtered sgRNAs with overlapping targets. This resulted in a total of 59,129 sgRNAs targeting
105 16,152 genes (~74% of all protein-coding genes that belong to families) (**Fig. 3a, Extended Data 1**). Of
106 the 59,129 sgRNAs, 98.7% target two to five genes; the rest target six to ten genes (**Fig. 3b**). This procedure
107 thus created a library of sgRNAs where every sgRNA targets multiple genes, and every gene is targeted by
108 multiple sgRNAs (**Fig. 3c, Supplementary Figure 1**).

109

110 **Construction of multi-targeted CRISPR sub-libraries for specific functional groups**

111 In an effort to increase the flexibility of the Multi-Knock library and enable targeted forward-genetics
112 screens, the 59,129 sgRNAs were classified into 10 groups according to the protein functions of their
113 putative target genes⁴, thus creating the following ten sub-libraries: transporters (TRP: 1,123 genes and
114 5,635 sgRNAs); protein kinases, protein phosphatases, receptors, and their ligands (PKR: 1,190 genes and
115 6,161 sgRNAs); transcription factors and other RNA and DNA binding proteins (TFB: 2,042 genes and
116 6,010 sgRNAs); proteins binding small molecules (BNO: 1,443 genes and 5,899 sgRNAs); proteins that
117 form or interact with protein complexes including stabilizing factors (CSI: 1,399 genes and 4,919 sgRNAs);
118 hydrolytic enzymes (enzyme classification [EC] class 3), excluding protein phosphatases (HEC: 1,438
119 genes and 6,215 sgRNAs); metabolic enzymes and enzymes (EC class2) that catalyze transfer reactions
120 (TEC: 1,041 genes and 4,145 sgRNAs); catalytically active proteins, mainly enzymes (PEC: 1,252 genes
121 and 4,975 sgRNAs); proteins with diverse functional annotations not found in the other categories (DMF:
122 1,343 genes and 5,000 sgRNAs); and proteins of unknown function or cannot be inferred (UNC: 3,881
123 genes and 10,170 sgRNAs) (**Fig. 3d, Supplementary Table 1**).

124 To facilitate the creation of the sub-libraries, adaptors of 38 to 47 nucleotides in length were added that
125 were unique to each sub-library (**Supplementary Table 2**). We amplified each sub-library using primers
126 complementary to the specific adaptors and used the Golden Gate method to clone the sgRNA sub-libraries
127 into the intronized zCas9 vector (pRPS5A:zCas9i). The intronized *Cas9* has 13 introns integrated into the
128 maize codon-optimized *Cas9*; these introns have a significant positive effect on *Cas9* genome editing
129 efficiency in *Arabidopsis*²³.

130 More than 2.0×10^5 clones of each sub-library (average coverage of 20-48× per sgRNA) growing on the
131 selection plates were harvested, and plasmid DNA from each sub-library was isolated. In order to evaluate

132 library quality, each sub-library was deep sequenced in a 150 paired-end mode (PE150). An ideal sgRNA
133 library should have < 0.5% undetected guides, and a skew ratio of less than 10²⁶. The sequencing data
134 showed that more than 98% of the designed sgRNAs in our libraries were present, with the exception of
135 sgRNAs in four sub-libraries (PKR, DMF, HEC, and UNC) that exhibited lower coverage percentages
136 (95.05%, 80.90%, 85.07%, and 71.58% coverage, respectively) (**Fig. 3e**). Importantly, the sgRNAs
137 frequencies in the sub-libraries showed a narrow bell-shaped distribution (skew < 2) (**Fig. 3e**), indicating
138 that no individual sgRNA were overly enriched. In addition, the effect of sgRNA cross-contamination
139 during library construction was evaluated using deep sequencing analysis. The data indicated that all sub-
140 libraries are highly specific (~99.9%), with the exception of the TEC sublibrary that showed significant
141 amplification (35%) of sgRNAs from CSI sublibrary (**Supplementary Figure 2**). With the exception of
142 the TEC sublibrary, all quality control analyses indicate that the Multi-Knock CRISPR sub-libraries are
143 ready to be used in plants for functional analysis.

144

145 **Multi-targeted transportome analysis**

146 To demonstrate that the Multi-Knock approach overcomes redundancy in forward-genetics screens *in*
147 *planta*, we chose to focus on the plant transportome using the TRP sub-library. Transporter families in
148 plants are generally large (e.g., 136 ABC members and 53 NPF members) and relatively uncharacterized
149 genetically²⁷. To expand the functional utility of our tool, we cloned the 5,635 sgRNA sequences into four
150 different Cas9 vectors to create independent TRP-sub-libraries, varying in their Cas9 type, the promoter driving
151 the Cas9, and resistance in plants: pRPS5A:zCas9i library described above, which results in high Cas9 genome-
152 editing activity in *Arabidopsis*²³; pRPS5A:Cas9 with OLE:CITRINE that carries BASTA resistance and allows
153 selection of Cas9 in seeds using a fluorescent Citrine protein²⁸ (**Supplementary Figure 3**); the commonly used
154 pUBI:Cas9 also imparts BASTA resistance^{29,30}; and pEC:Cas9 that carries kanamycin resistance and allows
155 mutation specifically in the egg cells to avoid somatic mutations³¹. The four sub-libraries were cloned and deep-
156 sequenced to evaluate sgRNA coverage and frequency. Coverage was higher than 98%, with a Gaussian
157 distribution for all four libraries (skew < 3) (**Fig. 4a**).

158 At least 2.2 x 10⁵ *Agrobacterium tumefaciens* clones of each TRP-sub-library were harvested and transformed into
159 *Arabidopsis* Col-0 plants yielding about 3,500 transgenic T1 plants (pUBI:Cas9, 500 lines; pEC:Cas9, 500 lines;
160 pRPS5A:Cas9 OLE:CITRINE, 500 lines; and pRPS5A:zCas9i 2,000 lines). To increase on-target mutagenesis
161 in plants, pUBI:Cas9, pEC:Cas9, and pRPS5A:zCas9i T1 plants were subjected to repeated mild heat stress
162 as previously described with slight modifications³². 2,000 T1 lines were collected individually for the
163 pRPS5A:zCas9i library. pUBI:Cas9, pEC:Cas9, and pRPS5A:Cas9 OLE:CITRINE libraries were each collected
164 in bulks of 10 plants. 1,200 independent T2 lines generated from the pRPS5A:zCas9i TRP sub-library were

165 screened in soil at 22°C under long-day conditions (16-h light and 8-h dark) using a high-throughput phenomics
166 system, evaluating photosynthesis-related parameters, thermal imaging, plant color, and shoot morphology.
167 Importantly, the screen recovered previously reported phenotypes of mutants affected in transporters. For
168 example, we isolated two independent lines with pale, bleached, and small-size shoots. Extracting DNA,
169 amplifying the sgRNA cassette, and sequencing revealed that they harbor the same sgRNA sequence,
170 putatively targeting *TOC132* and *TOC120* (Translocon Outer Complex proteins) (**Fig. 4b, Supplementary**
171 **Figure 4a**). Sanger sequencing of *TOC132* and *TOC120* revealed that frameshift mutations occurred at the
172 sgRNA target sites in these two genes (**Fig. 4b, Supplementary Figure 4b**). The similar phenotypes we
173 observed in two independent lines indeed mimicked the *toc132,toc120* double mutant phenotype that was
174 previously characterized³³. In addition, we identified phenotypes driven by two different sgRNAs targeting
175 two maltose transporters (MEX1 and MEX1-Like). The *mex1,mex1l* CRISPR double mutants phenotype
176 was enhanced compared to the previously described *mex1* single mutant³⁴ (**Fig. 4b, Supplementary Figure**
177 **5**). Plants targeting genes encoding two boron transporters (BOR1 and BOR2) were genotyped as double
178 *bor1,bor2* knockouts and had growth inhibition phenotypes (**Fig. 4b**), likely enhancing the *bor1-1* mutant-
179 plants³⁵. Unlike all other lines described here which were validated in T2 or T3 generations, the T1
180 generation *bor1,bor2* knockouts were sterile and did not produce seeds. Sequencing the sgRNA and their
181 putative target genes of additional lines showed edited DNA events in the majority of the targeting sites
182 (**Supplementary Figure 6**).

183 Many of the phenotypes we observed were driven by previously undescribed genes. For example, plants
184 expressing a single sgRNA resulted in deletions in *clc-a*, *clc-b* (Chloride Channels), or *vha-d1*, *vha-d2*
185 (Vacuolar-type H⁺ -ATPases) or *pup8*, *pup21* (Purin Permeases), all showing smaller rosette size than Col-
186 0 plants (**Fig. 4c**). Notably, while some of the mutations were homozygous, *TOC120*, *VHA-D2*, and *PUP8*
187 showed superimposed sequencing data. Chromatogram sequence deconvolution showed that *PUP8* is a
188 biallelic mutation (+T/+A) (**Fig. 4**). The data for *TOC120* and *VHA-D2* is less clear and could point to
189 biallelic or heterozygous mutations. At this stage, we do not know whether the phenotypes are a result of
190 an on-target activity, and further genetic validation is needed to rule out off-target effects. Such genetic
191 validation was carried out below for the *PUP* candidates. Notably, the Multi-Knock seed collection we
192 generated here is available to the community for any type of forward-genetic screen. Together, the results
193 demonstrate the strength of the Multi-Knock strategy in exposing novel mutant phenotypes.

194

195 **The Multi-Knock screen revealed partially redundant tonoplast-localized PUP cytokinin**
196 **transporters**

197 As noted above, the Multi-Knock transportome-scale screen identified a shoot growth inhibition phenotype
198 caused by *PUP8* and *PUP21* loss-of-function (**Fig. 4c**). The two unstudied proteins are members of the
199 PUP family, which consists of 21 genes (**Fig. 5a**). Most of the genes in the *PUP Arabidopsis* family have
200 not been characterized³⁶, but *PUP14* reportedly encodes for a plasma membrane cytokinin transporter³⁷. In
201 addition to plasma membrane-localized *PUP14*³⁷, *PUP1* and *PUP2* were also identified as cytokinin
202 transporters in *Arabidopsis*^{38,39}. In rice, OsPUP1 and OsPUP7 were shown to localize on the endoplasmic
203 reticulum (ER), while OsPUP4 was localized to the plasma membrane^{40,41}. Cytokinins are plant hormones
204 essential for meristem maintenance and additional physiological and developmental processes, such as cell
205 division, lateral root formation, leaf senescence, embryo development and adaptive responses to heat and
206 drought stresses⁴²⁻⁴⁴. Because cytokinin biosynthesis, catalyzed by isopentenyl-transferases, does not occur
207 throughout the plant but is limited to certain tissues, cytokinins are translocated through the plant by
208 diffusion and/or through active transport mechanisms^{36,45}. There is a complete genetic linkage between the
209 *PUP7*, *PUP21*, and *PUP8* genes, and phylogenetic analysis of *PUPs* in *Arabidopsis* showed that these three
210 genes form a monophyletic clade (**Fig. 5a**). Similar to *PUP8* and *PUP21*, the function of *PUP7* is unknown.

211 To characterize the activity of *PUP7*, *PUP21*, and *PUP8*, we isolated single *PUP7*, *PUP21*, and *PUP8* T-
212 DNA homozygous lines. The single *pup7* (SALK_084103) and *pup8* (SALK_137526) mutants showed no
213 morphological differences compared to Col-0. The *pup21* (GABI_288E11) mutant also did not show a
214 phenotype in the vegetative stage compared to Col-0, and presented only a mild plant height phenotype after
215 bolting (**Supplementary Figure 7**). To validate the potentially redundant on-target activity of *PUP7*,
216 *PUP21*, and *PUP8* as revealed by the *PUP8* and *PUP21* loss-of-function line (**Fig. 4c**), we cloned a
217 multiplexed CRISPR construct targeting *PUP7*, *PUP21*, and *PUP8* and obtained double (*CRISPR7/21*) and
218 triple (*CRISPR7/8/21*) mutants. Mutations were validated in generations T4 (*CRISPR7/8/21*) or T3
219 (*CRISPR7/21*). Both *CRISPR7/21* and *CRISPR7/8/21* showed frameshift mutations in their targets (**Fig.**
220 **5b**) that exhibited a small rosette size (**Fig. 5c,d**). The phenotype of the triple mutant (*CRISPR7/8/21*) was
221 enhanced compared to the *CRISPR7/21* double mutant and to the *CRISPR8/21* double mutant recovered
222 from the Multi-Knock screen (**Fig. 5 c,d**), indicating that *PUP7*, *PUP21*, and *PUP8* redundantly regulate
223 shoot growth. To further validate the on-target activity of *PUP7*, *PUP21*, and *PUP8* we generated a *PUP7*,
224 *PUP21*, and *PUP8* multi-targeted amiRNA line (*amiRNA7/8/21*). *amiRNA7/8/21* showed reduced
225 expression of *PUP7*, *PUP21*, and *PUP8* (**Supplementary Figure 8**). In agreement with the *CRISPR7/8/21*
226 triple mutant, the *amiRNA7/8/21* line also exhibited a small rosette size (**Fig. 5e,f**).

227 Cytokinin response was previously shown to regulate the spatial distribution of lateral organs along the
228 stem or phyllotaxis⁴⁶. We found a significant perturbed phyllotaxis phenotype with an increase in the
229 occurrence of abnormal angles between consecutive organs in *CRISPR7/8/21* and *amiRNA7/8/21* lines

230 (Fig. 5g-j). These results suggest that PUP7, PUP21, and PUP8 redundantly regulate shoot growth and
231 phyllotaxis.

232 To understand how PUP7, PUP8, and PUP21 function in cellular transport, we generated stable transgenic
233 plants that express PUP7, PUP8 and PUP21 fused with YFP under the control of the cauliflower mosaic
234 virus 35S promoter and evaluated the subcellular localization of these proteins in the root meristem
235 epidermis cells. PUP7 and PUP21 were localized to tonoplasts as indicated by co-localization with the vac-
236 uole marker⁴⁷, whereas PUP8 localized to the plasma membrane (Fig. 6a). We then performed
237 transport assays with the 3 proteins in *Xenopus laevis* oocytes using the cytokinin *trans*-zeatin (tZ). Based
238 on standard import assays and injection-based export assays, PUP8 was shown to be capable of bidirectional
239 cytokinin transport along the concentration gradient of cytokinin (Fig. 6b,c, Supplementary Figure 9).
240 The absence of transport activity of PUP7 and PUP21 in oocytes, which do not have vacuoles, likely results
241 from their mis-localization. In order to back up the oocyte data in a plant system, we expressed all three PUP
242 transporters in tobacco protoplasts and quantified tZ export after diffusion-based loading. Expression of
243 *PUP7* and *PUP21* resulted in significantly reduced cellular tZ export, while *PUP8* expression resulted in
244 enhanced tZ export (Fig. 6d,e). In order to demonstrate substrate specificity, we performed competition
245 experiments for PUP8 that allowed as a putative tZ exporter for direct competition of tZ uptake into
246 microsomal fractions. Addition of an excess of cold tZ significantly reduced transport activity of
247 radiolabelled tZ (Supplementary Figure 10).

248 To evaluate whether these PUP proteins are implicated in cytokinin transport and signaling, we monitored
249 the shoot apical meristem cytokinin response in Col-0 and *amiRNA7/8/21* plants using the synthetic
250 cytokinin-inducible reporter *TCS:Venus*⁴⁸. A severely reduced TCS signal was detected in *amiRNA7/8/21*
251 vegetative and inflorescence shoot apical meristems compared to controls (Fig. 6f-i). The TCS domain at
252 the center of the SAM and in flowers was also much narrower in *amiRNA7/8/21* compared to wild type
253 (Fig. 6f,g), thus demonstrating also a change in the spatial distribution of cytokinin responses in the SAM.
254 Overall, these results indicated that tonoplast-localized PUP7 and PUP21 can act as vacuolar cytokinin
255 importers, while plasma membrane-localized PUP8 is required for cytokinin export. This cytokinin
256 transport activity is required to establish the spatial pattern of cytokinin signaling within the SAM, thus
257 regulating shoot growth and phyllotaxis. However, since directional transport activity of PUP8, and
258 possibly of PUP7 and PUP21, depends on cytoplasmic (or apoplastic) cytokinin levels, it is possible that
259 their transport directionality might change spatially. Taken together, our discovery of these novel cytokinin
260 transporters was made possible through the simultaneous targeting of the multiple *PUP* genes.

261

262 **Discussion**

263 The large number of gene families in *Arabidopsis* results in high levels of functional redundancy⁴⁹. In recent
264 years, genome-scale amiRNA collections have been developed in *Arabidopsis* and used for forward-genetic
265 screening to identify hidden phenotypes masked by redundant homologous genes^{4,9}. However, this strategy
266 generally results in incomplete knockout phenotypes. The CRISPR/Cas9 system is a simple, effective
267 method for generating targeted heritable mutations in the genome and has recently enabled large-scale
268 knockout mutant libraries of single genes to be generated for forward-genetic screens in mammalian^{50,51}
269 and plant systems¹⁵⁻¹⁹. An important advantage of the CRISPR/Cas9 method is its capacity to
270 simultaneously target multiple genes, whether they are genetically linked or not. In this study, we developed
271 a novel genome-scale approach with the ability to simultaneously target several genes within the same gene
272 family and applied it in *Arabidopsis*. This forward-genetic strategy overcomes functional redundancy and
273 enables flexible screening, ranging from a specific functional subgroup to the entire genome. We reported
274 here on six lines with reproducible phenotypes and validated the respective editing of the target genes. It is
275 important to note that we have observed dozens of novel phenotypes (i.e., by screening for differences in
276 shoot size, color, shape and photosynthesis-related parameters) that we have not followed up with detailed
277 experiments. As the intronized-CAS9 efficiency is above 70%^{23,52}, we project that the rate-limiting step is
278 not the library or the intronized-CAS9 efficiency, but rather the genetic screen setup and cost-effective
279 genotyping strategies. Overall, the approach we developed and the library we constructed should allow a
280 broad spectrum of functional screens to be readily carried out, thereby significantly impacting current
281 genetic analyses in plants.

282 The present strategy constructed the Multi-Knock tool using a single sgRNA design to optimally target
283 multiple genes. We expect that with the anticipated progress in the field, future developments of the Multi-
284 Knock approach could utilize sgRNA multiplexing. While constructing a genome-scale sgRNA
285 multiplexed CRISPR library is at present technically challenging (currently limited by the base-pair length
286 of pooled oligo libraries containing thousands of sgRNAs), a breakthrough in the field will increase the
287 overall targeting efficiency and coverage. In addition, the current Multi-Knock tool is designed to target
288 redundancy resulting from multiple proteins with highly similar sequences carrying overlapping activity
289 and having highly similar coding sequences. However, Multi-Knock will not reveal redundancy resulting
290 from overlapping pathways (diverse gene families with overlapping transcriptional or biochemical
291 activities). The development of a multiplexing Multi-Knock library would naturally uncover redundant
292 pathways, by allocating each sgRNA to target a different set of (one or more) homologous proteins.

293 As a proof-of-concept that Multi-Knock can identify novel gene functions, we identified the first cytokinin
294 tonoplast transporters in plants. There are discrepancies in published data concerning the subcellular
295 localization of cytokinin receptors and the cellular site of cytokinin perception. In different studies,

296 cytokinin receptors have been shown to localize to the endoplasmic reticulum membrane⁵³⁻⁵⁶ and to the
297 plasma membrane³⁷. Recently, two independent groups described multiple sites of cytokinin perception at
298 plasma and endoplasmic reticulum membranes^{57,58}. We speculate that the tonoplast localization of PUP7
299 and PUP21 may facilitate the movement of cytokinins into vacuoles, thereby lowering the availability of
300 cytokinins in the cytoplasm and/or the ER. However, it is important to note that injection or diffusion-based
301 tZ loading might promote PUP-mediated tZ transport from high to low concentration in both *Xenopus* and
302 tobacco, respectively. Under *in vivo* conditions, it is possible that PUP transport directionalities may also
303 shift, depending on local cytokinin concentrations or electrochemical gradient changes.

304 The direction of both uni- and symporters was previously shown to be reversible *in vitro* depending on the
305 direction of the electrochemical gradient of their substrate and/or symported ion⁵⁹⁻⁶². For example, PUP8
306 and the SWEET (SUGARS WILL EVENTUALLY BE EXPORTED TRANSPORTER) transporters were
307 both identified using import-based screens but were shown to be bidirectional in *Xenopus* oocytes^{61,62}.
308 Lastly, PUP8 was shown to possess phlorizin transport capability via an import-based screen of > 600
309 *Arabidopsis* transporters and also shown to be bidirectional. Phlorizin is a dihydrochalcone abundantly
310 found in apples, which indicates that PUP8 might have acquired additional substrates in plants⁶¹. It is thus
311 intriguing to speculate that dual-directional PUPs activity in different cell types, possibly among shoot
312 apical meristem zones, regulates cytokinin response by mediating sub-cellular cytokinin homeostasis. The
313 tonoplast-dependent cytokinin transport may also have an impact on cell-to-cell cytokinin movement. Such
314 coordination among a network of plasma membrane and tonoplast transporters might determine the
315 cytokinin fluxes within the cell and within tissues. Therefore, the tonoplast localization of PUP7 and PUP21
316 identified here adds another level of regulation to the response mediated by endoplasmic reticulum-
317 localized cytokinin receptors.

318 Using the Multi-Knock strategy, we demonstrated partially redundant functions of PUP8, PUP7, and
319 PUP21 in cytokinin transport either across the plasma membrane or into the vacuole, which would both
320 lead to reduced cytoplasmic cytokinin levels. In all cases, the genes are genetically linked and functionally
321 redundant, emphasizing the power and need of Multi-Knock as a genome-scale multi-targeted approach. It
322 is common that evolutionary conserved transporter families in plants share redundant activities and are
323 genetically linked, suggesting recent gene-duplication events. For example, in five ABCB auxin
324 transporters (ABCB15-22) of the same phylogenetic branch, their simultaneous knockout using Cas9
325 exposed their redundant activity⁶³. Additional examples are the genetically linked and redundant activities
326 of ABCB6 and ABCB20 in auxin transport⁹ and of ABCG17 and ABCG18 in ABA transport⁶⁴. We predict
327 that future genetic screens, utilizing approaches as the one developed here, will expose the activities of
328 many genetically linked and redundant genes.

329 Saturated screens allows to observe the same phenotype in multiple independent lines, creating multiple
330 alleles and partially omitting false positive candidate lines. Here, we screened ~1,200 independent T2 lines
331 from the CRISPR TRP library, which contains 5,635 sgRNAs, meaning there is a very low chance of
332 identifying multiple independent lines containing sgRNAs that target the same genes. However, we
333 successfully isolated independent lines for *toc120,toc132*, and *mex1,mex11*, likely because of their strong
334 visible phenotypes. One way to tackle this issue is to screen for high-throughput phenotypes as carried out
335 in the mammalian field using cell culture⁵¹. However, such screens do not benefit from the strength of
336 screening *in planta*. Another way one can isolate multiple events and screen a X10 coverage, saturated
337 population, is to bulk 10 or 100 lines together (for example, 56K lines covering 5,635 sgRNAs). This allows
338 rapid screening and increases the chance of identifying the same sgRNA multiple times. At the same time,
339 this approach has drawbacks as it is harder to pick up on minor phenotypes. An alternative approach to
340 tackle the issue of saturated screens is to generate smaller libraries that cover specific groups of limited size,
341 thereby increasing the chance of observing multiple lines directed towards the same set of genes.

342 Following successful phenotyping and genotyping of Multi-Knock T2 plants, just as in any other genetic
343 approach (e.g., use of alkylating agents, T-DNA, amiRNA), it is critical to validate that the phenotype is
344 indeed driven by the specific mutation. Ursache et al., reported that an *Agrobacteria* mix, containing
345 multiple constructs, could result in the integration of more than one construct per plant⁵². Furthermore,
346 Jacobs et al., reported that transient expression of sgRNAs in tomato might cause CRISPR mediated
347 mutations in respective target gene¹⁵, both leading to possible off-target effects. One way to address these
348 obstacles and reveal possible on/off-targets is to use the SMAP multiplex PCR amplicon tool to genotype
349 putative target sites⁶⁵. Addition methods to validate on-target activity may include complementation lines
350 to demonstrate phenotype rescue, or generate multiple independent mutant lines (such as a combination of
351 T-DNA lines or, in cases of genetic linkage, sgRNAs or amiRNA) that present the same phenotype.

352 Here we presented the Multi-Knock tool and validated its use for gene function discovery in *Arabidopsis*.
353 This genome-scale multi-targeted mutagenesis system may also be applied to other plant species and
354 utilized for next-generation breeding programs to uncover hidden genetic variations. However, in contrast
355 to flower-dip transformation in *Arabidopsis*, large-scale *Agrobacterium*-mediated plant transformations in
356 crops is still a bottleneck due to low transformation efficiency and the requirement for labor-intensive tissue
357 culture. Thus, once transformation efficiency is enhanced, for example, using sgRNA delivery by viral
358 vectors^{66,67} or nanoparticle-based carriers^{68,69}, we foresee that the Multi-Knock approach could be readily
359 employed in many other plant species. Notably, the Multi-Knock tool requires high-quality information on
360 gene space. While high-quality sequenced genomes of most important crops, and dozens of other plants,
361 are already available, this could be an issue for less studied plant species. A possible alternative in such

362 cases is to extract the gene-space via deep sequencing of the transcriptome, albeit limiting the off-target
363 search to coding regions only.

364

365 **Materials and Methods**

366 **Plant material and growth conditions.** All *Arabidopsis* plants were derived from the Columbia ecotype
367 and grown in dedicated growth rooms under long-day conditions (16 h light/ 8 h dark) at 22 °C. *Arabidopsis*
368 Col-0 plants were transformed using *Agrobacterium* strains (GV3101) by the flower dip method⁷⁰.

372 **Multi-targeted sgRNA design.** All 9,350 gene families in the *Arabidopsis thaliana* genome, encompassing
373 27,416 genes, were downloaded from the PLAZA 3.0 plant comparative genomics database²⁴. Genes
374 belonging to the mitochondrial and chloroplast genomes were filtered out, as well as families with a single
375 family member, leaving 3,892 families of size 2 or more that together encompassed 21,798 genes. The
376 CRISPyS algorithm was then applied to each family while accounting for the homologous relationships
377 within each family. Specifically, given a family of genes, a gene tree was reconstructed using a hierarchical
378 clustering algorithm⁷¹, which clusters the genes according to their sequence similarity. The s^{Ω} design
379 strategy of CRISPyS was then recursively applied to each subgroup induced by the gene tree to find the
380 optimal sgRNAs for targeting the desired subfamily. CRISPyS was applied using the CFD (Cutting
381 Frequency Determination) score⁷² as the scoring function with targeting efficacy threshold of $\Omega = 0.55$ and
382 $k = 12$ as the threshold for the number of polymorphic sites. The number of sgRNAs per each subgroup of
383 genes in a given gene tree was limited to 200. The potential sgRNA targets were allowed only for the first
384 two-thirds of the coding sequence. Since CRISPyS could assign the same sgRNAs for different subgroups
385 of homologous genes, where one subgroup is a subset of the other one (for example, assuming that
386 $\{g_1, g_2, g_3\}$ is a subset of homologous genes, and s is an sgRNA that targets this subgroup of genes, the
387 same sgRNA s can also be found for $\{g_1, g_2\}$), we considered only one occurrence of the sgRNA.

388 For each remaining sgRNA, a genome-wide off-target detection was applied. In the context of gene-family
389 cleavage, an off-target is defined as a potential genomic target that is outside the specified gene family,
390 while on-targets are nuclear targets that reside within the family, even though some mismatches may occur
391 between them and the examined sgRNA. To this end, given a specified sgRNA, the Burrows-Wheeler
392 Aligner (BWA)⁷³ was applied to the *Arabidopsis thaliana* genome (PLAZA v3) to identify potential nuclear
393 hits. BWA was executed with the command "bwa aln", with the following parameters: -N, -l 20, -i 0, -n 5,
394 -o 0, -d 3, -k 4, -M 0, -O 1000000, -E 0, thus allowing searching for targets with at most four mismatches
395 and no gaps. Only hits that reside within protein-coding exons were considered off-targets. A potential
396 sgRNA was filtered if it was inferred to cleave an off-target with a CFD score higher than 0.33. We then
397 applied an additional filtering procedure, where we tested the remained sgRNAs for overlapping target

398 regions. A given sgRNA was removed if all its targets overlapped with those of a second potential sgRNA,
399 and the CFD scores of most of these targets were lower. A sgRNA s_1 is defined to overlap with sgRNA s_2
400 if the positions of all its targets overlap with those of s_2 in at least 10% of the aligned region (i.e., 2 bp).

410 **CRISPR/Cas9 vectors**

411 To generate the pRPS5A:Cas9 OLE:CITRINE plasmid, Site-Directed Mutagenesis (NEB-E0554S), was used to
412 eliminate the 3 BsaI sites within the OLE:CITRINE sequence, using the following primers: Fwd-
413 ATGGGCCGAGACAGGGACCAGTACCAGATGTCCGGAC Rev-
414 CATCGGGTACTGGTCCCTGCCGATGATATCGTGATGG. The BsaI sites are required for the Golden gate
415 CRISPR library cloning. Next, OLE:CITRINE was cut and ligated from pJET into pRPS5A:Cas9 vector using
416 MluI and BamHI restriction enzymes. pUBI:Cas9 was generated as described previously²⁹. pRPS5A:zCAS9i
417 (Addgene ID: AGM55261)²³ and pEC:Cas9 (Addgene ID: pHEE401)³¹ were purchased from Addgene.

418 **Construction of Multi-Knock, multi-targeted CRISPR libraries.** The 20-nucleotide sgRNA target sites
419 were appended with the specific adaptors and BsaI sites (**Supplementary Table 2**). Synthesis of the 59,129
420 DNA oligonucleotides (total yield: 500 ng) corresponding to the sgRNAs was performed by Twist
421 Bioscience. A stock solution of oligo pool was prepared by resuspending in 10 mM Tris buffer, pH 8.0 to
422 a concentration of at least 20 ng/ μ l. The single-stranded oligonucleotide pool was converted to double-
423 stranded DNA by PCR using the high-fidelity Phusion polymerase (NEB) using 12 to 15 cycles of PCR to
424 avoid introducing PCR bias. PCR was conducted using the following conditions: 98 °C for 30 s; 15 cycles
425 of 98 °C for 30 s, 60 °C for 30 s, and 72 °C for 15 s; and a final extension at 72 °C for 10 min. For each
426 family pool, about 6 tubes of 50 μ l-volume amplification reactions with a total of 15 ng single-stranded
427 oligonucleotide pool as a template and the specific primers for adaptors (**Supplementary Table 3**) were
428 used, and the PCR products were purified with a NucleoSpin Gel and PCR clean up Kit (Macherey-Nagel).

429 The purified DNA products were digested with BsaI restriction enzyme and ligated into the desired Cas9
430 expression constructs using the Golden Gate cloning method. Golden Gate assembly was performed as
431 follows: 35 cycles of 37 °C for 5 min and 16 °C for 5 min; 50 °C for 20 min; and 80 °C for 20 min. Four
432 20- μ l ligation reactions were combined, and 20 bacterial transformations were carried out using 4 μ l of
433 ligation reaction and 50 μ l Top10 chemically competent *E. coli* per transformation according to the
434 manufacturer's instructions. The 20 transformations were combined and plated onto seven LB agar plates
435 (145 x 20 mm, Greiner Bio-one) supplemented with the relevant antibiotics. Colonies were validated using
436 colony PCR and Sanger sequencing individually, then bacteria from all plates were scraped off and
437 combined. The plasmid DNA was purified with a Plasmid Maxi kit (Qiagen) to produce the CRISPR
438 libraries. In order to verify these plasmid pools, PCR products amplified with the primers listed in
439 **Supplementary Table 4** from the CRISPR libraries were sequenced on an Illumina NovaSeq 6000 with

440 the PE150 mode. Eight 50 μ l amplification reactions using the high-fidelity Phusion DNA Polymerase
441 (NEB) were set up. PCR was conducted using the following conditions: 98 $^{\circ}$ C for 30 s; 30 cycles of 98 $^{\circ}$ C
442 for 30 s, 60 $^{\circ}$ C for 30 s, and 72 $^{\circ}$ C for 15 s; and a final extension at 72 $^{\circ}$ C for 10 min. PCR products were
443 purified with a NucleoSpin Gel and PCR clean-up Kit (Macherey-Nagel). At least 1.5 μ g PCR products per
444 each sub-library were sent to Novogene for deep-sequencing.

445 The number of reads per sgRNA sequence was quantified from the raw sequencing data using the Biopython
446 package in the Python programming language. A list of sgRNAs comprising the library was loaded into
447 python. A loop was performed where each one of the sgRNAs in the list was compared against the raw
448 deep-sequencing data in FASTA using the Biopython package and quantified the number of reads where
449 the specific sgRNA appeared. The sgRNA and its read number were written into a new data frame.

450 **Generation of four transportome CRISPR libraries.** The four transportome CRISPR plasmids were
451 transformed into *Agrobacterium tumefaciens* strain GV3101 using electroporation. In brief, for each library,
452 around 20 tubes of GV3101 competent cells (80 μ l) were incubated on ice with \sim 1 μ g plasmid in each tube
453 for 5 min and electroporated using a MicroPulser (Bio-Rad Laboratories; 2.2 kV, 5.9 ms). Immediately
454 after electroporation, 700 μ l LB medium was added, and samples were shaken for 1.5-2 h at 28 $^{\circ}$ C.
455 *Agrobacterium* was then plated on LB agar plates (145 x 20 mm, Greiner Bio-one) containing the relevant
456 antibiotics for 2 days at 28 $^{\circ}$ C in the dark. Each *Agrobacterium* transportome CRISPR library was
457 transformed into six trays of *Arabidopsis* Col-0 plants. T1 Seeds were collected in bulk. After transformant
458 plant selection, transgenic plants for each transportome CRISPR library were propagated, and T2 seeds
459 were collected.

460 ***Arabidopsis* transformation and heat-shock treatment.** The *Agrobacterium* colonies from all plates were
461 scraped off and added into 1 L LB medium with 25 μ g/ml gentamycin, 25 μ g/ml rifampicin, and vector-
462 specific antibiotic, followed by incubation at 28 $^{\circ}$ C for 16-24 hours. *Agrobacterium* was harvested by
463 centrifugation for 10 min at 5,500 rpm, the supernatant was discarded, and the bacteria pellet was
464 resuspended in \sim 400 ml inoculation medium containing 0.5 x MS (Duchefa Biochemie), 5.0% sucrose, and
465 0.05% Tween-20 (Sigma-Aldrich). *Arabidopsis* flowers were then sprayed with the bacterial solution. After
466 spraying, plants were kept in the dark overnight and grown until siliques ripened and dried. T1 seeds were
467 collected in bulk. The T1 seeds of the pEC:zCas9 library were sown on MS media containing hygromycin
468 (25 μ g/ml) for the transformant plant selection, whereas the T1 seeds of the other three transportome
469 CRISPR libraries were sown on soil and sprayed with BASTA for selection at the age of 2 weeks. T1
470 transgenic plants were subjected to repeated heat stress treatments as previously described with slight
471 modifications³² (with the exception of pRPS5A:Cas9 OLE:CITRINE). The plants that were subjected to
472 heat stress were treated as follows: After resistance selection and 4 days of acclimation to the soil, the

473 seedlings were transferred to growth chambers at 32 °C for 24 h, followed by a 48 h recovery at 22 °C (3-
474 day period). This heat stress cycle was performed four times during the vegetative phase of growth. The
475 plants were then grown at 22 °C from that point on.

476 **CRISPR/CAS9 and amiRNA cloning.** The 20 nt protospacer (CTCTACTTTCTCCCTCATCT) was
477 picked to target PUP7 (AT4G18197), PUP8 (AT4G18195) and PUP21 (AT4G18205) at once. The oligos
478 (FW: attgCTCTACTTTCTCCCTCATCT; REV: aaacAGATGAGGGAGAAAGTAGAG) were annealed
479 and cloned into the pRPS5A:zCAS9i (Addgene: AGM55261) using the Golden Gate cloning method. In
480 brief, the oligos were incubated at 95°C for 5 mins and cooled at RT for 20 mins. The annealed oligos and
481 the pRPS5A:zCAS9i were added in the following reaction (20 µl): 3µl of annealed oligos; ~150 ng of CAS9
482 vector; 1 µl T4 ligase (400,000 units/ml, NEB); 1 µl BsaI-HF v2 (20,000 units/ml, NEB); Cutsmart buffer
483 (NEB) and T4 ligase buffer (NEB). Golden Gate assembly was performed as follows: 35 cycles of 37 °C
484 for 5 min and 16 °C for 5 min; 50 °C for 20 min; and 80 °C for 20 min. 1/10 of the reaction was transformed
485 into *E.coli* DH5α.

486 To generate the 35S:amiRNA-PUP7/8/21 vector, the amiRNA319 backbone sequence with miR targeting
487 *PUP7*, *PUP8* and *PUP21* (MiR-sense: TATCATGGAAAACACTGTCCTG) was synthesized by Syntezza
488 Bioscience Ltd. and cloned into the pH2GW7 destination vector using the Gateway system.

489 **Genotyping.** To identify the sgRNA of transgenic plants, genomic DNA from young leaf tissue was
490 extracted by grinding 1-2 leaves into 400 µl Extraction Buffer (200 mM Tris-HCl, pH 8.0, 250 mM NaCl,
491 25 mM EDTA, and 0.5% SDS). After 1-min centrifugation at 13,000 rpm, 300 µl supernatant was
492 transferred to a new Eppendorf tube and mixed with 300 µl isopropanol, followed by centrifugation for 10
493 min at maximum speed. The supernatant was removed and the DNA pellets were washed with 70% ethanol
494 and then resuspended in 50 µl of water. The PCR amplified using the primers listed in **Supplementary**
495 **Table 4 and 5** was identified using Sanger sequencing.

496 T-DNA lines for the single mutants, listed in **Supplementary Table 6**, were ordered from Gabi Kat
497 (<https://www.gabi-kat.de>) and The *Arabidopsis* Information Resource (<https://www.arabidopsis.org/>).
498 Primers for the T-DNA genotyping were designed using the T-DNA Primer Design Tool powered by
499 Genome Express Browser Server (<http://signal.salk.edu/tdnaprimers.2.html>). Homozygous mutants were
500 selected by PCR performed with primers listed in **Supplementary Table 6**.

501 **Phenomics.** Morphological and photosynthesis parameters were analyzed with the PlantScreen™
502 Phenotyping System, Photon Systems Instruments (PSI), Czech Republic. Plants were sowed in PSI
503 standard pots and imaged at day 25.

504 **35S:YFP-PUPs cloning.** PUP7 genomic DNA, PUP8-CDS and PUP21-CDS were amplified with Phusion
505 High-fidelity Polymerase (NEB) using the primers list in **Supplementary Table 7**. PUP7 genomic
506 sequence with intron, PUP8, and PUP21 coding regions was cloned into pENTER/D-TOPO (Invitrogen
507 K2400), verified by sequencing, and subsequently cloned into the binary destination vector (pH7WGY2)
508 using LR Gateway reaction (Invitrogen 11791). *p35S:YFP-PUP7*, *p35S:YFP-PUP8*, and *p35S:YFP-*
509 *PUP21* were generated using the pH7WGY2 vector and were selected using spectinomycin in *Escherichia*
510 *coli* and hygromycin in plants.

511 **Microscopy imaging.** Seedlings were stained in 10 mg L⁻¹ propidium iodide (PI) for 5 min and rinsed in
512 water for 30 s. Confocal microscopy was performed using a Zeiss LSM780 inverted confocal microscope
513 equipped with a 20×/0.8 M27 objective lens. YFP and CFP were excited using an argon-ion laser, whereas
514 PI was excited using a diode laser. Emissions were detected sequentially with ZEN to prevent crosstalk
515 between fluorophores. YFP was excited at 514 nm, CFP at 458 nm, and PI at 561 nm. Fluorescence emission
516 was measured at 517-561 nm (YFP), 523-552 (CITRINE), 463-517 nm (CFP), and 588-718 nm (PI).

517 **Expression and cytokinin transport assays in *Xenopus* oocytes.** Coding DNA sequences of PUP7, PUP8
518 and PUP21 were cloned into *Xenopus laevis* oocyte expression vector pNB1u using USER cloning
519 technique as described previously⁷⁴. DNA template for in vitro transcription was generated by PCR using
520 Phusion High-Fidelity DNA Polymerase (NEB) using forward primer (5'-
521 AATTAACCCTCACTAAAGGGTTGTAATACGACTCACTATAGGG-3') and reverse primer (5'-
522 TTTTTTTTTTTTTTTTTTTTTTTTTTTTTTTTATACTCAAGCTAGCCTCGAG-3'). The PCR products
523 were purified using the E.Z.N.A. Cycle Pure Kit (Omega Bio-tek). Capped complementary RNA (cRNA)
524 was in vitro transcribed using the mMessage mMachine T7 Kit (Invitrogen AM1344) following the
525 manufacturer's instructions.

526 *X. laevis* oocytes (stage V or VI) were purchased from Ecocyte Bioscience (Germany). Oocytes were
527 injected with 15 ng of PUP7, PUP8, or PUP21 cRNA (or 50.6 nl nuclease-free water as mock control) using
528 a Drummond NANOJECT II (Drummond Scientific Company, Broomall Pennsylvania). The injected
529 oocytes were incubated for 3 days at 16°C in a kulori buffer (90 mM NaCl, 1 mM KCl, 1 mM MgCl₂, 1
530 mM CaCl₂, 5 mM Hepes pH 7.4) supplemented with gentamycin (100 µg/ml).

531 Three days after cRNA injection, the injection-based export assay was performed. Oocytes were injected
532 with 23nl of 2mM trans-zeatin (tZ) and then oocytes were incubated in a group of 3 oocytes in 150 ul kulori
533 buffer (90 mM NaCl, 1 mM KCl, 1 mM MgCl₂, 1 mM CaCl₂, 10 mM MES pH 5.5) for 150 min. After
534 150 min, the oocytes and their respective external medium were harvested separately for intracellular and
535 extracellular tZ quantification, respectively. The samples were homogenized with 50% methanol and then
536 stored at -20°C overnight. Subsequently, the extracts were spun down at 15,000g for 15 min at 4°C and the

537 supernatant was diluted with water, filtered through a 0.22 µm polyvinylidene difluoride-based filter plate
538 (MSGVN2250, Merck Millipore), and analyzed by analytical liquid chromatography coupled to mass
539 spectrometry (LC-MS/MS). Export of tZ was calculated as follows: ((amount of tZ in the medium at time
540 t=150 min)/(amount of tZ in the oocyte at time t=150 min + amount of tZ in the medium at time t=150
541 min))*100%.

542 Uptake assay was performed as described previously⁷⁵, with some modifications. A mixture of three types
543 of cytokinin (*trans*-zeatin (tZ), *trans*-zeatin riboside (tZR), and isopentenyl adenosine (iPR)) with a final
544 concentration of each type at 10 or 100 µM were used. Three days after cRNA injection, oocytes were
545 preincubated in kulori buffer (pH 5.5 or pH 8.5) for five minutes, and then the oocytes were incubated in
546 10 or 100 µM of cytokinin mix (tZ, tZR and iPR) containing kulori buffer (pH 5.5 or pH 8.5) for 60 min.
547 Oocytes were then washed four times in kulori buffer (pH 5.5 or pH 8.5) and homogenized with 50 %
548 methanol. Subsequent extraction and oocyte sample preparation was performed as described above.

549 **Cytokinin quantification by LC-MS/MS.** Samples were 100-fold diluted with deionized water and
550 subjected to analysis by liquid chromatography coupled to mass spectrometry. Chromatography was
551 performed on an Advance UHPLC system (Bruker, Bremen, Germany). Separation was achieved on a
552 Kinetex 1.7u XB-C18 column (100 x 2.1 mm, 1.7 µm, 100 Å, Phenomenex, Torrance, CA, USA). Formic
553 acid (0.05%) in water and acetonitrile (supplied with 0.05% formic acid) were employed as mobile phases
554 A and B, respectively. The elution profile was: 0-0.1 min, 5% B; 0.1-1.0 min, 5-45 % B; 1.0-3.0 min 45-
555 100 % B, 3.0-3.5 min 100 % B, 3.5-3.55 min, 100-5 % B and 3.55-4.7 min 5 % B. The mobile phase flow
556 rate was 400 µl min⁻¹. The column temperature was maintained at 40°C. The liquid chromatography was
557 coupled to an EVOQ Elite TripleQuadrupole mass spectrometer (Bruker, Bremen, Germany) equipped with
558 an electrospray ion source (ESI). The instrument parameters were optimized by infusion experiments with
559 pure standards. The ion spray voltage was maintained at +5000 V in positive mode. Cone temperature was
560 set to 350 °C and cone gas to 20 psi. The heated probe temperature was set to 250 °C and probe gas flow
561 to 50 psi. Nebulizing gas was set to 60 psi and collision gas to 1.6 mTorr. Nitrogen was used as a probe and
562 nebulizing gas and argon as collision gas. The active exhaust was constantly on. Multiple reaction
563 monitoring (MRM) was used to monitor analyte precursor ion → fragment ion transitions. MRM transitions
564 were adapted from literature⁷⁶. Detailed values for mass transitions and references are listed in
565 **Supplementary Table 8.** Both Q1 and Q3 quadrupoles were maintained at unit resolution. Bruker MS
566 Workstation software (Version 8.2.1, Bruker, Bremen, Germany) was used for data acquisition and
567 processing. Linearity in ionization efficiencies were verified by analyzing dilution series.

568 **Tobacco cytokinin transport assays.** For protoplast export experiments, *35S:YFP:PUPs* were transiently
569 expressed in *N. benthamiana* leaf tissues by *Agrobacterium tumefaciens*-mediated transfection, protoplasts
570 were prepared and [¹⁴C]*tZ* and [³H]BA export was quantified simultaneously as described previously⁷⁷.
571 For microsomal uptake experiments, *35S:YFP:PUP8* was expressed in *N. benthamiana* leaf tissue by
572 *Agrobacterium tumefaciens*-mediated transfection, and microsomes were prepared and assayed as
573 described previously³⁷. In short, ¹⁴C-labelled *tZ* was added to 300 µg of 25 microsomes in the presence of
574 5 mM ATP to yield a final concentration of 1 µM [¹⁴C]*tZ*. For substrate competition assays, unlabelled
575 substrate was included in the transport buffer at a 100-fold excess. After 10 s of incubation at 20°C, aliquots
576 of 100 µl were vacuum-filtered and subjected to scintillation counting. Means and standard error of means
577 of at least four independent experiments with four technical replicates each are represented.

578 **Measurements of *TCS:Venus* responses.** Leaf or floral primordia were removed with the help of a fine
579 forceps (Swiss No.5) under a Nikon SMZ 745 stereoscope. Dissected shoot apices were inserted into Apex
580 Culture Medium (1/2 x MS medium (Duchefa), 1% sucrose, 1% agarose, 2 mM MES (Sigma), 1x vitamin
581 solution (myo-Inositol 100 mg/L, nicotinic acid 1 mg/L, pyridoxine hydrochloride 1 mg/L, thiamine
582 hydrochloride 10 mg/L, glycine 2 mg/L), 250 nM N6-Benzyladenine)). Confocal images were obtained
583 with a Zeiss LSM 700 microscope equipped with a water-dipping lens (W Plan-Apochromat 40x/1.0 DIC).
584 Venus and auto-fluorescence (chlorophyll A) were excited by both 488 nm laser with emission range at
585 300-550 nm and 664-800 nm, respectively. Images were processed and analyzed using Fiji (fiji.sc)
586 software.

587 **Phylogenetic tree.** A phylogenetic tree of *Arabidopsis* PUP family members, based on protein sequences,
588 was constructed using Phylogeny.fr (<http://www.phylogeny.fr/>)⁷⁸ with “one-click” mode. The previously
589 unreported PUP9 protein (AT4G18220), a close paralog of PUP10, was identified and added to the
590 phylogenetic analysis (**Fig. 5a**).

591 **Measurements of silique divergence angles.** Angles separating successive siliques on the main
592 inflorescence stem were quantified using a protractor as previously described⁷⁹. The divergence angle was
593 measured between the insertion points of two successive floral pedicels. Phyllotaxy orientation can be either
594 clockwise or anticlockwise.

595

596 **Acknowledgments**

597 We thank Bruno Müller (University of Zurich, Switzerland) for sharing *TCS:VENUS* seeds. **Funding:** This
598 work was supported by grants from the Israel Science Foundation (2378/19 and 3419/20 to E.S.), the
599 Human Frontier Science Program (HFSP—RGY0075/2015 and HFSP—LIY000540/2020 to E.S., H.H.N.-

600 E. and Z.M.B.), Danmarks Grundforskningsfond (DNRF99 to H.H.N.-E.), the European Research Council
601 (757683-RobustHormoneTrans to E.S.), the PBC postdoctoral fellowship (to Y.H.), and by the Swiss
602 National Funds (31003A-165877/1 to M.G.).

603

604 **Author contributions**

605 Y.H. and E.S. conceived and designed the study and wrote the manuscript. Y.H. performed the research.
606 P.P. assisted in cloning the Multi-Knock libraries and with PUP genetics. O.P. cloned and characterized the
607 PUP amiRNA and PUP reporter lines. A.S., G.H. and O.C. carried out the Multi-Knock sgRNA library
608 bioinformatics design and analysis. Z.M.B. performed transport assays in the *Xenopus* oocytes. J.B. carried
609 out the Multi-Knock sgRNA library deep-sequencing analysis. S.B. cloned the OLE:CITRINE Cas9 vector.
610 B.S. carried out the *TCS:VENUS* assays. L.C. performed the tobacco transport assays. C.C. performed the
611 LC-MS analysis. Y.Z. assisted in the PUP genes discovery. M.T. assisted in the library screen. D.W assisted
612 in the Multi-Knock sgRNA library design. A.A. provided the UBI:Cas9 vector. H.H.N.-E., M.G., T.V., and
613 I.M. designed and supervised the work and edited the manuscript. All authors discussed the results and
614 commented on the manuscript.

615

616 **Competing interests:** The authors declare that they have no competing interests.

617

618 **Data, code and materials availability:** All the data and supporting the findings of this study are available
619 within the article and the Supplementary Materials. All source codes used to generate the library are
620 available upon request.

621

622 **References**

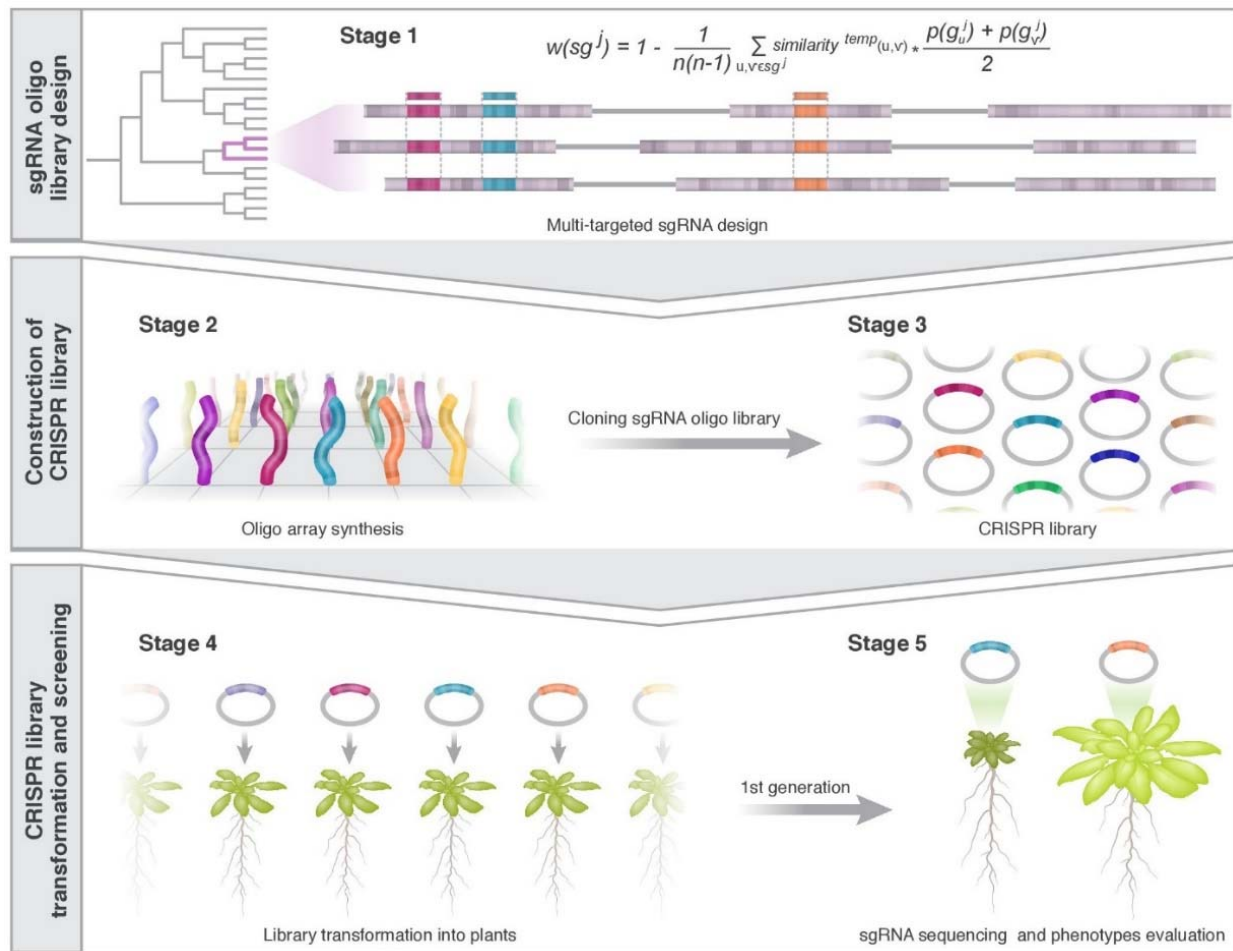
- 623 1. Panchy, N., Lehti-Shiu, M. & Shiu, S. H. Evolution of gene duplication in plants. *Plant Physiol.*
624 **171**, 2294–2316 (2016).
- 625 2. Rensing, S. A. Gene duplication as a driver of plant morphogenetic evolution. *Curr. Opin. Plant*
626 *Biol.* **17**, 43–48 (2014).
- 627 3. Alonso, J. M. *et al.* Genome-wide insertional mutagenesis of *Arabidopsis thaliana*. *Science.* **301**,
628 653–657 (2003).
- 629 4. Hauser, F. *et al.* A genomic-scale artificial MicroRNA library as a tool to investigate the
630 functionally redundant gene space in *Arabidopsis*. *Plant Cell* **25**, 2848–2863 (2013).
- 631 5. Henry, I. M. *et al.* Efficient genome-wide detection and cataloging of EMS-induced mutations
632 using Exome capture and next-generation sequencing. *Plant Cell* **26**, 1382–1397 (2014).
- 633 6. Tal, I. *et al.* The *Arabidopsis* NPF3 protein is a GA transporter. *Nat. Commun.* **7**, 11486 (2016).

- 634 7. Tang, X. *et al.* A Single Transcript CRISPR-Cas9 System for Efficient Genome Editing in Plants.
635 *Mol. Plant* **9**, 1088–1091 (2016).
- 636 8. Wang, L. *et al.* Construction of a genomewide RNAi mutant library in rice. *Plant Biotechnol. J.*
637 **11**, 997–1005 (2013).
- 638 9. Zhang, Y. *et al.* A transportome-scale amiRNA-based screen identifies redundant roles of
639 Arabidopsis ABCB6 and ABCB20 in auxin transport. *Nat. Commun.* **9**, 4204 (2018).
- 640 10. Li, Z. *et al.* Gene duplicability of core genes is highly consistent across all angiosperms. *Plant Cell*
641 **28**, 326–344 (2015).
- 642 11. Lu, X. *et al.* Gene-Indexed Mutations in Maize. *Mol. Plant* **11**, 496–504 (2018).
- 643 12. Gaillochet, C., Develtere, W. & Jacobs, T. B. CRISPR screens in plants: Approaches, guidelines,
644 and future prospects. *Plant Cell* **33**, 794–813 (2021).
- 645 13. Chen, K., Wang, Y., Zhang, R., Zhang, H. & Gao, C. CRISPR/Cas Genome Editing and Precision
646 Plant Breeding in Agriculture. *Annu. Rev. Plant Biol.* **70**, 667–697 (2019).
- 647 14. Mali, P. *et al.* RNA-guided human genome engineering via Cas9. *Science.* **339**, 823–826 (2013).
- 648 15. Jacobs, T. B., Zhang, N., Patel, D. & Martin, G. B. Generation of a collection of mutant tomato
649 lines using pooled CRISPR libraries. *Plant Physiol.* **174**, 2023–2037 (2017).
- 650 16. Chen, K. *et al.* A FLASH pipeline for arrayed CRISPR library construction and the gene function
651 discovery of rice receptor-like kinases. *Mol. Plant* **15**, 243–257 (2021).
- 652 17. Liu, H. J. *et al.* High-throughput CRISPR/Cas9 mutagenesis streamlines trait gene identification in
653 maize. *Plant Cell* **32**, 1397–1413 (2020).
- 654 18. Lu, Y. *et al.* Genome-wide Targeted Mutagenesis in Rice Using the CRISPR/Cas9 System. *Mol.*
655 *Plant* **10**, 1242–1245 (2017).
- 656 19. Meng, X. *et al.* Construction of a Genome-Wide Mutant Library in Rice Using CRISPR/Cas9.
657 *Mol. Plant* **10**, 1238–1241 (2017).
- 658 20. Bai, M. *et al.* Generation of a multiplex mutagenesis population via pooled CRISPR-Cas9 in soya
659 bean. *Plant Biotechnol. J.* **18**, 721–731 (2020).
- 660 21. Ramadan, M. *et al.* Efficient CRISPR/Cas9 mediated Pooled-sgRNAs assembly accelerates
661 targeting multiple genes related to male sterility in cotton. *Plant Methods* **17**, 1–13 (2021).
- 662 22. Lorenzo, C. D. *et al.* BREEDIT: a multiplex genome editing strategy to improve complex
663 quantitative traits in maize. *Plant Cell* (2022).
- 664 23. Grützner, R. *et al.* High-efficiency genome editing in plants mediated by a Cas9 gene containing
665 multiple introns. *Plant Commun.* **2**, 1–15 (2021).
- 666 24. Proost, S. *et al.* PLAZA 3.0: An access point for plant comparative genomics. *Nucleic Acids Res.*
667 **43**, D974–D981 (2015).
- 668 25. Hyams, G. *et al.* CRISPys: Optimal sgRNA Design for Editing Multiple Members of a Gene
669 Family Using the CRISPR System. *J. Mol. Biol.* **430**, 2184–2195 (2018).
- 670 26. Joung, J. *et al.* Genome-scale CRISPR-Cas9 knockout and transcriptional activation screening.
671 *Nat. Protoc.* **12**, 828–863 (2017).

- 672 27. Kang, J. *et al.* Plant ABC Transporters. *Arab. B.* **9**, e0153 (2011).
- 673 28. Tsutsui, H. & Higashiyama, T. PKAMA-ITACHI vectors for highly efficient CRISPR/Cas9-
674 mediated gene knockout in *Arabidopsis thaliana*. *Plant Cell Physiol.* **58**, 46–56 (2017).
- 675 29. Sussholz, O., Pizarro, L., Schuster, S. & Avni, A. SIRLK-like is a malectin-like domain protein
676 affecting localization and abundance of LeEIX2 receptor resulting in suppression of EIX-induced
677 immune responses. *Plant J.* **104**, 1369–1381 (2020).
- 678 30. Fauser, F., Schiml, S. & Puchta, H. Both CRISPR/Cas-based nucleases and nickases can be used
679 efficiently for genome engineering in *Arabidopsis thaliana*. *Plant J.* **79**, 348–359 (2014).
- 680 31. Wang, Z. P. *et al.* Egg cell-specific promoter-controlled CRISPR/Cas9 efficiently generates
681 homozygous mutants for multiple target genes in *Arabidopsis* in a single generation. *Genome Biol.*
682 **16**, 1–12 (2015).
- 683 32. LeBlanc, C. *et al.* Increased efficiency of targeted mutagenesis by CRISPR/Cas9 in plants using
684 heat stress. *Plant J.* **93**, 377–386 (2018).
- 685 33. Kubis, S. *et al.* Functional specialization amongst the *Arabidopsis* Toc159 Family of chloroplast
686 protein import receptors. *Plant Cell* **16**, 2059–2077 (2004).
- 687 34. Niittylä, T. *et al.* A Previously Unknown Maltose Transporter Essential for Starch Degradation in
688 Leaves. *Science.* **303**, 87–89 (2004).
- 689 35. Takano, J. *et al.* *Arabidopsis* boron transporter for xylem loading. *Nature* **420**, 337–340 (2002).
- 690 36. Kang, J., Lee, Y., Sakakibara, H. & Martinoia, E. Cytokinin Transporters: GO and STOP in
691 Signaling. *Trends Plant Sci.* **22**, 455–461 (2017).
- 692 37. Zürcher, E., Liu, J., Di Donato, M., Geisler, M. & Müller, B. Plant development regulated by
693 cytokinin sinks. *Science.* **353**, 1027–1030 (2016).
- 694 38. Bürkle, L. *et al.* Transport of cytokinins mediated by purine transporters of the PUP family
695 expressed in phloem, hydathodes, and pollen of *Arabidopsis*. *Plant J.* **34**, 13–26 (2003).
- 696 39. Gillissen, B. *et al.* A new family of high-affinity transporters for adenine, cytosine, and purine
697 derivatives in *Arabidopsis*. *Plant Cell* **12**, 291–300 (2000).
- 698 40. Xiao, Y. *et al.* Endoplasmic Reticulum-Localized PURINE PERMEASE1 Regulates Plant Height
699 and Grain Weight by Modulating Cytokinin Distribution in Rice. *Front. Plant Sci.* **11**, 1–12
700 (2020).
- 701 41. Xiao, Y. *et al.* Big Grain3, encoding a purine permease, regulates grain size via modulating
702 cytokinin transport in rice. *J. Integr. Plant Biol.* **61**, 581–597 (2019).
- 703 42. Perilli, S., Moubayidin, L. & Sabatini, S. The molecular basis of cytokinin function. *Curr. Opin.*
704 *Plant Biol.* **13**, 21–26 (2010).
- 705 43. Wybouw, B. & De Rybel, B. Cytokinin – A Developing Story. *Trends Plant Sci.* **24**, 177–185
706 (2019).
- 707 44. Ha, S., Vankova, R., Yamaguchi-Shinozaki, K., Shinozaki, K. & Tran, L. S. P. Cytokinins:
708 Metabolism and function in plant adaptation to environmental stresses. *Trends Plant Sci.* **17**, 172–
709 179 (2012).
- 710 45. Sakakibara, H. Cytokinins: Activity, biosynthesis, and translocation. *Annu. Rev. Plant Biol.* **57**,

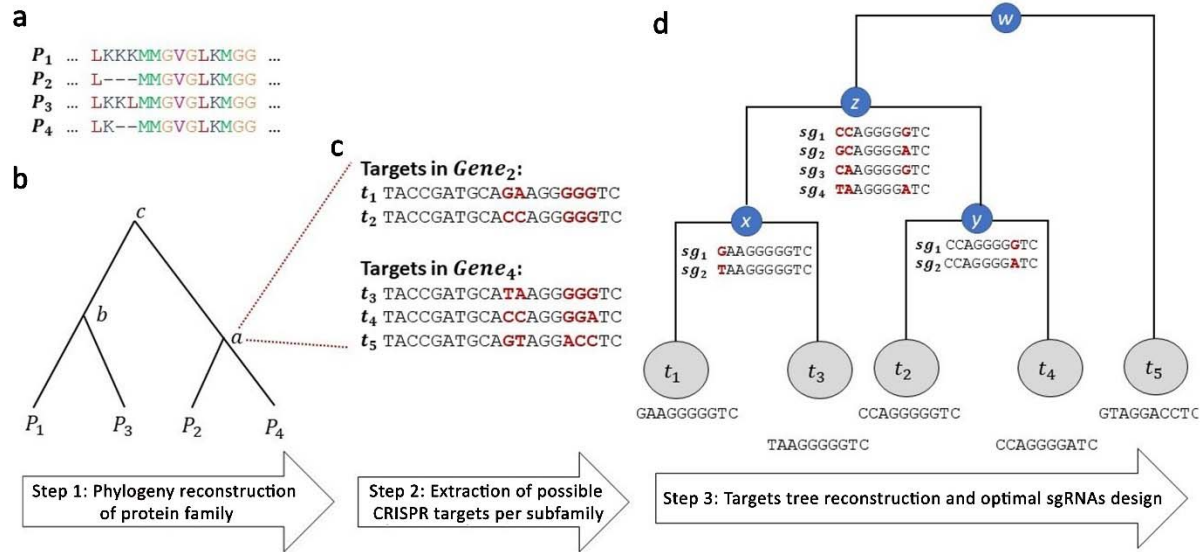
- 711 431–449 (2006).
- 712 46. Besnard, F. *et al.* Cytokinin signalling inhibitory fields provide robustness to phyllotaxis. *Nature*
713 **505**, 417–421 (2014).
- 714 47. Nelson, B. K., Cai, X. & Nebenführ, A. A multicolored set of in vivo organelle markers for co-
715 localization studies in Arabidopsis and other plants. *Plant J.* **51**, 1126–1136 (2007).
- 716 48. Bruno, M. & Jen, S. Cytokinin and auxin interplay in root stem-cell specification during early
717 embryogenesis. *Nature* **4**, 1094–1097 (2008).
- 718 49. O'Malley, R. C. & Ecker, J. R. Linking genotype to phenotype using the Arabidopsis unimutant
719 collection. *Plant J.* **61**, 928–940 (2010).
- 720 50. Park, R. J. *et al.* A genome-wide CRISPR screen identifies a restricted set of HIV host dependency
721 factors. *Nat. Genet.* **49**, 193–203 (2017).
- 722 51. Wang, T., Wei, J. J., Sabatini, D. M. & Lander, E. S. Genetic screens in human cells using the
723 CRISPR-Cas9 system. *Science.* **343**, 80–84 (2014).
- 724 52. Ursache, R., Fujita, S., Déneraud, V. & Geldner, N. Combined fluorescent seed selection and
725 multiplex CRISPR/Cas9 assembly for fast generation of multiple Arabidopsis mutants. *Plant*
726 *methods*, **17**. 111 (2021).
- 727 53. Caesar, K. *et al.* Evidence for the localization of the Arabidopsis cytokinin receptors AHK3 and
728 AHK4 in the endoplasmic reticulum. *J. Exp. Bot.* **62**, 5571–5580 (2011).
- 729 54. Wulfetange, K. *et al.* The cytokinin receptors of arabidopsis are located mainly to the endoplasmic
730 reticulum. *Plant Physiol.* **156**, 1808–1818 (2011).
- 731 55. Lomin, S. N., Yonekura-Sakakibara, K., Romanov, G. A. & Sakakibara, H. Ligand-binding
732 properties and subcellular localization of maize cytokinin receptors. *J. Exp. Bot.* **62**, 5149–5159
733 (2011).
- 734 56. Ding, W. *et al.* Isolation, characterization and transcriptome analysis of a cytokinin receptor
735 mutant *osckt1* in rice. *Front. Plant Sci.* **8**, 1–13 (2017).
- 736 57. Antoniadi, I. *et al.* Cell-surface receptors enable perception of extracellular cytokinins. *Nat.*
737 *Commun.* **11**, 4284 (2020).
- 738 58. Kubiasová, K. *et al.* Cytokinin fluoroprobe reveals multiple sites of cytokinin perception at plasma
739 membrane and endoplasmic reticulum. *Nat. Commun.* **11**, 1–11 (2020).
- 740 59. Carpaneto, A. *et al.* Phloem-localized, proton-coupled sucrose carrier ZmSUT1 mediates sucrose
741 efflux under the control of the sucrose gradient and the proton motive force. *J. Biol. Chem.* **280**,
742 21437–21443 (2005).
- 743 60. Léran, S. *et al.* Arabidopsis NRT1.1 is a bidirectional transporter involved in root-to-shoot Nitrate
744 translocation. *Mol. Plant* **6**, 1984–1987 (2013).
- 745 61. Mussa Belew, Z. *et al.* Identification and characterization of phlorizin transporter from
746 Arabidopsis 1 thaliana and its application for phlorizin production in Saccharomyces cerevisiae.
747 *bioRxiv* (2020).
- 748 62. Chen, L. Q. *et al.* Sugar transporters for intercellular exchange and nutrition of pathogens. *Nature*
749 **468**, 527–532 (2010).

- 750 63. Chen, J. *et al.* ABCB-mediated auxin transport in outer root tissues regulates lateral root spacing
751 in Arabidopsis. *bioRxiv* (2020).
- 752 64. Zhang, Y. *et al.* ABA homeostasis and long-distance translocation are redundantly regulated by
753 ABCG ABA importers. *Sci. Adv.* **7**, 1–18 (2021).
- 754 65. Develtere, W. *et al.* SMAP design: A multiplex PCR amplicon and gRNA design tool to screen for
755 natural and CRISPR-induced genetic variation. *bioRxiv* (2022).
- 756 66. Ellison, E. E. *et al.* Multiplexed heritable gene editing using RNA viruses and mobile single guide
757 RNAs. *Nat. Plants* **6**, 620–624 (2020).
- 758 67. Wang, M. *et al.* Gene Targeting by Homology-Directed Repair in Rice Using a Geminivirus-
759 Based CRISPR/Cas9 System. *Mol. Plant* **10**, 1007–1010 (2017).
- 760 68. Martin-Ortigosa, S. *et al.* Mesoporous silica nanoparticle-mediated intracellular cre protein
761 delivery for maize genome editing via loxP site excision. *Plant Physiol.* **164**, 537–547 (2014).
- 762 69. Mitter, N. *et al.* Clay nanosheets for topical delivery of RNAi for sustained protection against
763 plant viruses. *Nat. Plants* **3**, (2017).
- 764 70. Clough, S. J. & Bent, A. F. Floral dip : a simplified method for Agrobacterium-mediated
765 transformation of Arabidopsis thaliana. **16**, 735–743 (1999).
- 766 71. Gronau, I. & Moran, S. Optimal implementations of UPGMA and other common clustering
767 algorithms. *Inf. Process. Lett.* **104**, 205–210 (2007).
- 768 72. Doench, J. G. *et al.* Optimized sgRNA design to maximize activity and minimize off-target effects
769 of CRISPR-Cas9. *Nat. Biotechnol.* **34**, 184–191 (2016).
- 770 73. Li, H. & Durbin, R. Fast and accurate short read alignment with Burrows-Wheeler transform.
771 *Bioinformatics* **25**, 1754–1760 (2009).
- 772 74. Nour-Eldin, H. H., Hansen, B. G., Nørholm, M. H. H., Jensen, J. K. & Halkier, B. A. Advancing
773 uracil-excision based cloning towards an ideal technique for cloning PCR fragments. *Nucleic
774 Acids Res.* **34**, (2006).
- 775 75. Jørgensen, M., Crocoll, C., Halkier, B. & Nour-Eldin, H. Uptake Assays in *Xenopus laevis*
776 Oocytes Using Liquid Chromatography-mass Spectrometry to Detect Transport Activity. *Bio-
777 Protocol* **7**, 1–13 (2017).
- 778 76. Ionescu, I. A. *et al.* Transcriptome and metabolite changes during hydrogen cyanamide-induced
779 floral bud break in sweet cherry. *Front. Plant Sci.* **8**, 1–17 (2017).
- 780 77. Jarzyniak, K. *et al.* Early stages of legume–rhizobia symbiosis are controlled by ABCG-mediated
781 transport of active cytokinins. *Nat. Plants* **7**, (2021).
- 782 78. Dereeper, A. *et al.* Phylogeny.fr: robust phylogenetic analysis for the non-specialist. *Nucleic Acids
783 Res.* **36**, 465–469 (2008).
- 784 79. Prasad, K. *et al.* Arabidopsis PLETHORA transcription factors control phyllotaxis. *Curr. Biol.* **21**,
785 1123–1128 (2011).
- 786
- 787



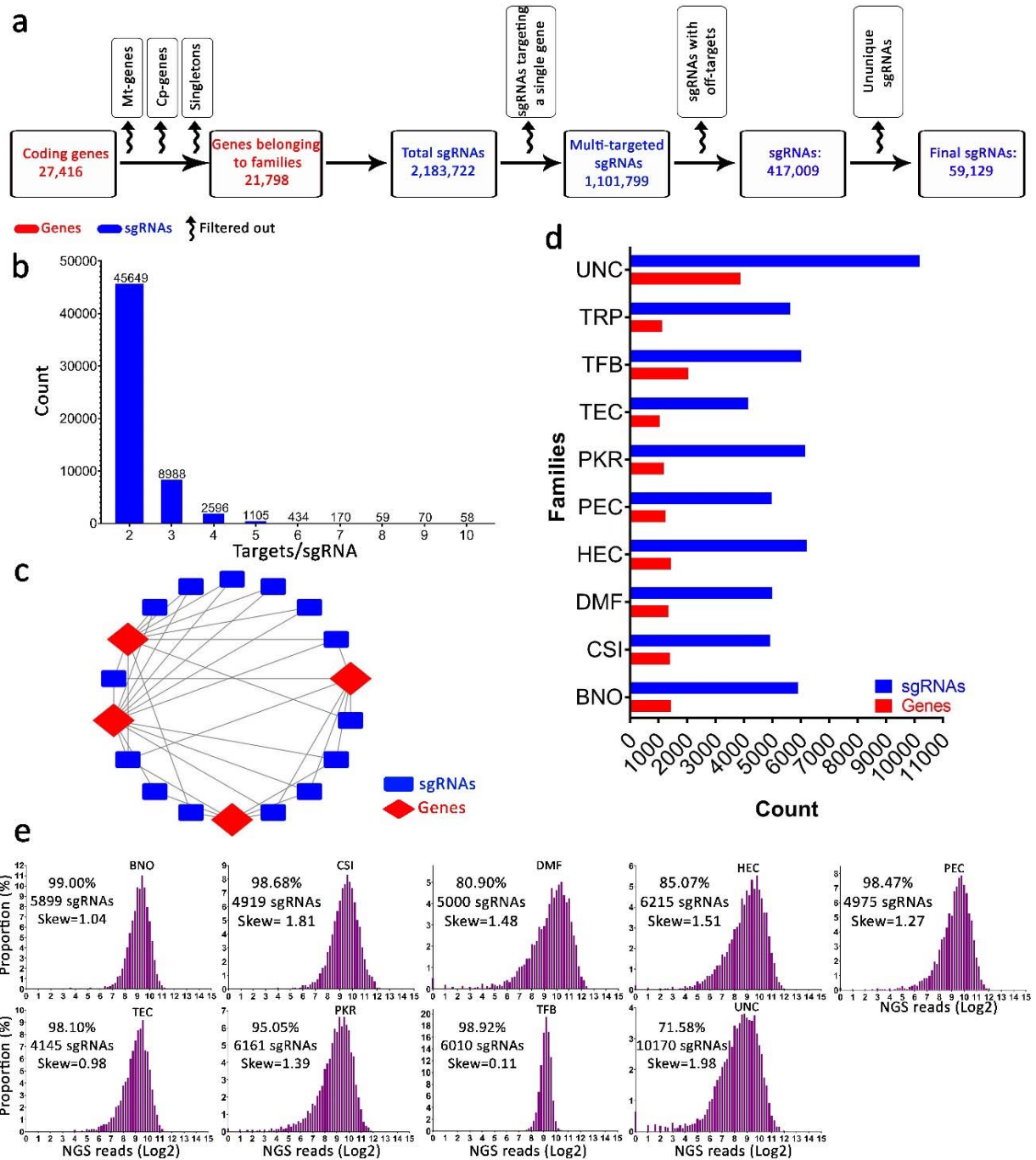
788

789 **Fig. 1: Overview of the Multi-Knock, genome-scale, multi-targeted CRISPR platform.** Stage 1: Multi-
 790 targeted sgRNAs were designed to target multiple genes (coding sequences) from the same family. The
 791 *Arabidopsis* genome was clustered into gene families and multiple sgRNAs were designed to target each node
 792 using the CRISPys algorithm. Stages 2 and 3: sgRNA sub-library sequences were synthesized, amplified, and
 793 cloned into CRISPR/Cas9 vectors. Stage 4: The pooled CRISPR library was introduced into *Agrobacterium* and
 794 transformed into *Arabidopsis* to generate stable lines. Each plant expresses a single sgRNA, targeting a clade of 2
 795 to 10 genes from the same family. Stage 5: A phenotypic forward genetic screen was conducted. Candidate lines
 796 were genotyped for sgRNAs and targets.
 797



798

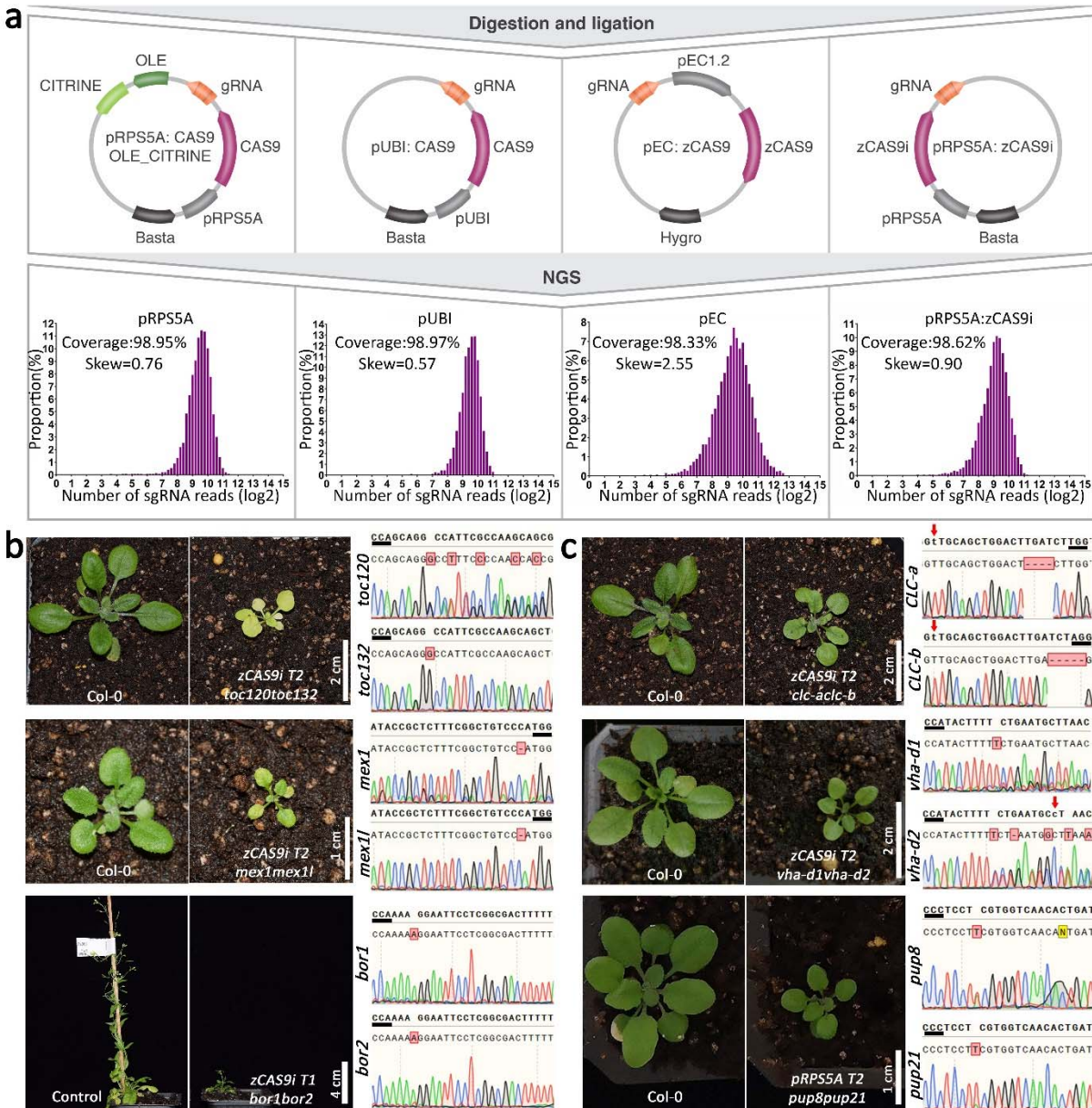
799 **Fig. 2: An overview of sgRNA design strategy for gene families.** **a**, For each gene family, the multiple
800 alignments of the respective protein sequences is computed. P stands for protein, and letters indicate amino
801 acids. **b**, A phylogenetic tree is constructed based on the sequence similarity of the protein sequences.
802 Optimal sgRNAs for each subgroup of genes, which are induced by internal nodes in the tree (marked by
803 lowercase letters a - c), are then designed. **c**, For each subfamily of genes, and illustrated here for node a , all
804 potential CRISPR target sites are extracted. In this case, the subfamily induced by node a includes two
805 genes (g_2 and g_4 , encoding for proteins P_2 and P_4 , respectively). Typically, each gene contains dozens of
806 possible targets. For simplicity, only five targets are presented. Nucleotide positions that are identical in all
807 targets are colored in black, while the polymorphic sites are colored in red and are in bold type. **d**, A tree
808 of the target sites is constructed based on sequence similarity among the targets while accounting for
809 CRISPR-specific characteristics. sgRNA candidates are constructed for each internal node, where all
810 combinations of the polymorphic sites are considered (marked in red), and the ones with the highest editing
811 efficacy to target the considered subgroup of genes are chosen. For simplicity, only a few candidates
812 (denoted by s_i) are shown for each internal node. Assuming that the cutoff of the number of polymorphic
813 sites k is 4, the search of sgRNA candidates stops at node z . In practice, k was set to 12 polymorphic sites.



814

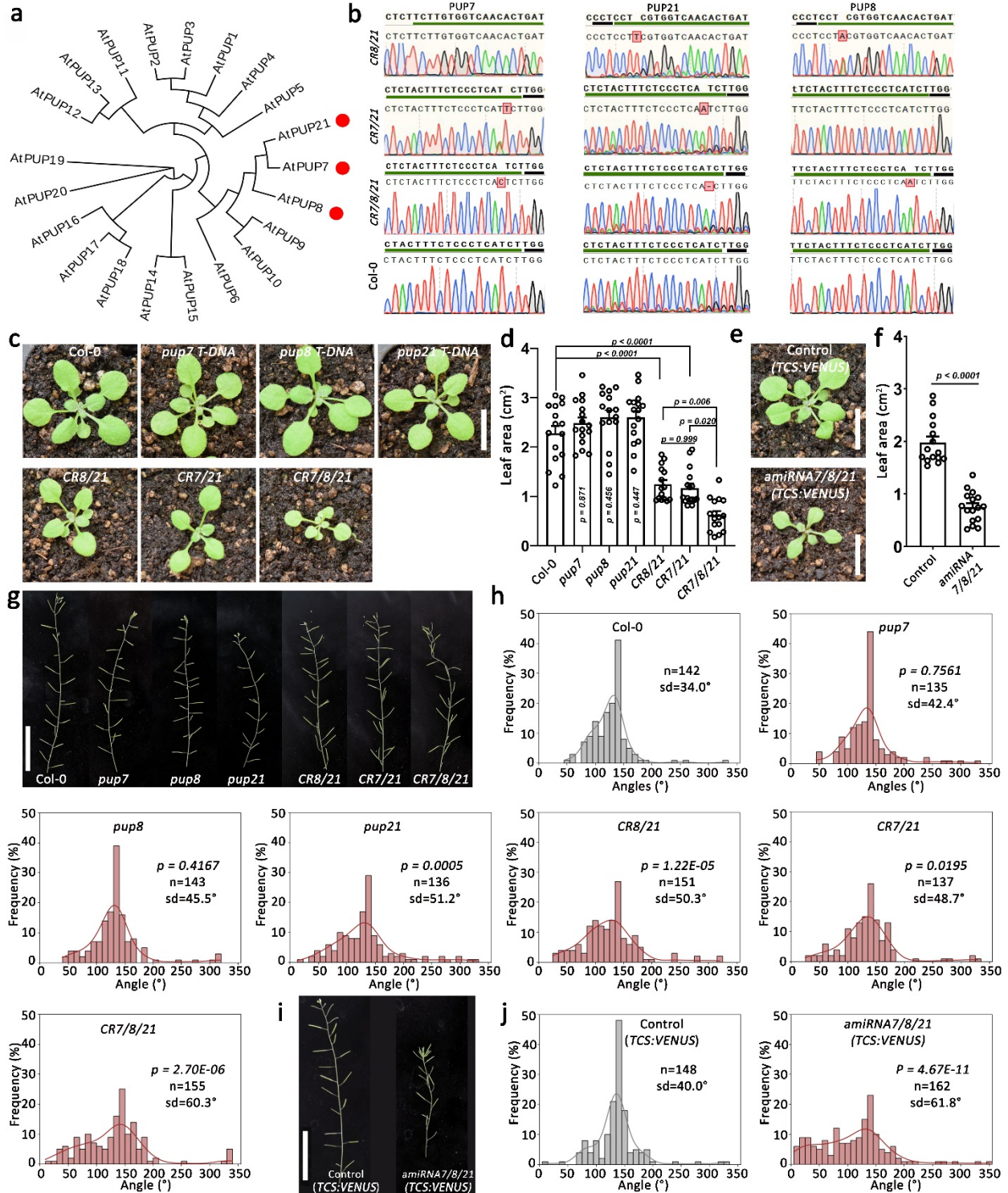
815 **Fig. 3: Multi-targeted genome-scale sgRNA design and construction.** **a**, Schematic illustration of the
 816 computational workflow used to design the Multi-Knock sgRNA library. A filtering process yielded a selection
 817 of 59,129 sgRNAs targeting 16,152 genes (~74% of all coding genes belonging to families). The red color
 818 represents coding genes, blue color represents sgRNAs, and curved arrows represent filtering steps. Abbreviations:
 819 Mt-genes, mitochondrial genes; Cp-genes, chloroplast genes; Singletons, genes that do not belong to a family. **b**,
 820 Histogram showing the number of genes targeted by individual sgRNAs. **c**, Representative sgRNA-target network
 821 in the CRISPR library. Genes are targeted by multiple sgRNAs, and sgRNAs target multiple genes. **d**, Total number
 822 of sgRNAs and target genes in each functional sub-library. **e**, Deep-sequencing data of sgRNAs in individual sub-
 823 libraries. Columns indicate the distribution of sgRNAs. Coverage is indicated for each group. TRP (transporters);

824 PKR (protein kinases, protein phosphatases, receptors, and their ligands); TFB (transcription factors and
825 other RNA and DNA binding proteins); BNO (proteins binding small molecules); CSI (proteins that form
826 or interact with protein complexes including stabilizing factors); HEC (hydrolytic enzymes); TEC
827 (metabolic enzymes and enzymes that catalyze transfer reactions); PEC (catalytically active proteins,
828 mainly enzymes); DMF (proteins with diverse functional annotations not found in the other categories);
829 and UNC (proteins of unknown function or cannot be inferred).
830



831

832 **Fig. 4: Transportome-specific Multi-Knock screen.** **a**, To create independent sub-libraries, 5,635 sgRNAs, each
 833 targeting 2 to 10 transporters from the same family, were amplified and cloned into four different Cas9 vectors to
 834 create pRPS5A:Cas9 (OLE:CITRINE), pUBI:Cas9, pEC:Cas9, and pRPS5A:zCas9i sub-libraries. Graphs show
 835 coverage and frequency based on next-generation sequencing of the four sub-libraries. The four libraries were
 836 transformed into Col-0 plants yielding 3,500 transgenic T1 plants. **b**, Photographs show representative phenotypes
 837 of TRP Multi-Knock proof-of-concept lines. From top to bottom are Col-0 and plant expressing sgRNA targeting
 838 *toc120* and *toc132* (scale bar = 2 cm), Col-0 and plant expressing sgRNA targeting *mex1* and *mex11* (scale bar = 1
 839 cm), and control *DR5:VENUS* plant and the T1 plant harboring sgRNA targeting *bor1* and *bor2* (scale bar = 4 cm).
 840 Chromatograms show the types of mutations. Red arrows indicate the mismatches between sgRNA and target
 841 sequence. PAM is marked with a black underline. **c**, Images show lines with abnormal phenotypes that had not
 842 previously been described: from top to bottom adjacent to Col-0 control are plants expressing sgRNA targeting *clc-*
 843 *a* and *clc-b* (scale bar = 2 cm), *vha-d1* and *vha-d2* (scale bar = 2 cm), and *pup8* and *pup21* (scale bar = 1 cm).
 844 Chromatograms show the type of mutations. Red arrows indicate the mismatches between sgRNA and target
 845 sequence. PAM is marked with a black underline.



846
847

848 **Fig. 5: PUP7, 8, and 21 redundantly regulate shoot growth and phyllotaxis.** **a**, Phylogenetic tree of *Arabidopsis*
 849 PUP family based on amino acid sequences. Red dots indicate proteins coded by putative *CR7/8/21* target genes.
 850 **b**, Chromatograms showing the types of mutations in the *CR8/21* (T3 generation), *CR7/21* (T3 generation) and
 851 *CR7/8/21* (T4 generation) lines as identified by sequencing. *CR8/21* and *CR7/21* stand for CRISPR double mutant
 852 *pup8/21* and *pup7/21*, respectively; *CR7/8/21* stands for CRISPR triple mutant *pup7/8/21*. PAM is underlined in

853 black; 20-bp sgRNA is underlined in green. The sgRNA in line *CR8/21* was not designed to target PUP7 as it does
854 not contain a respective PAM sequence. **c**, Shown are representative images of 18-day-old WT (Col-0), the T-
855 DNA single *pup7*, *pup8*, *pup21* mutants, the double *pup8pup21* (*CR8/21*) (T3 generation), double
856 *pup7pup21* (*CR7/21*) (T3 generation), and the triple *pup7pup8pup21* CRISPR mutant (*CR7/8/21*) (T4
857 generation). Scale bar = 1 cm. **d**, Quantification of genotypes shown in (c). Shown are means (\pm SE). *p* value
858 in ordinary one-way ANOVA is indicated for each analysis. Col-0, *pup7*, *pup21*, *CR7/21* and *CR7/8/21*:
859 *n*=16; *pup8* and *CR8/21*: *n*=15. **e**, Shown are representative images of 18-day-old Control (*TCS:VENUS*)
860 and *amiRNA7/8/21* (*TCS:VENUS* background). *amiRNA7/8/21* stands for amiRNA knockdown *PUP7/8/21*.
861 Scale bar = 1 cm. **f**, Quantification of genotypes shown in (e). Shown are means (\pm SE). *p* value two tailed
862 *t* test is indicated. *n* = 15 (Control); *n* = 16 (*amiRNA7/8/21*). **g**, Phyllotaxis patterns in inflorescences stem of
863 wild-type (Col-0), single T-DNA insertion mutants, *CR8/21*, *CR7/21* and *CR7/8/21*. Scale bar = 5 cm. **h**, Silique
864 divergence angle distribution in inflorescences of Col-0, *pup* single mutants, *CR8/21*, *CR7/21* and *CR7/8/21*. *P*-
865 value, *n* number and standard deviation (sd) are indicated for each analysis. *P*-value was extracted using Fligner-
866 Killeen test for equality of variance. **i**, Phyllotaxis patterns in inflorescence stem of control (*TCS:VENUS*) and
867 *amiRNA7/8/21* mutant. *amiRNA7/8/21* stands for amiRNA triple *PUP7/8/21* knockdown. Scale bar = 5 cm. **j**,
868 Distribution of divergence angle frequencies between successive siliques in control and *amiRNA7/8/21* stems. *p*
869 value Fligner-Killeen test for equality of variance is indicated for each analysis.

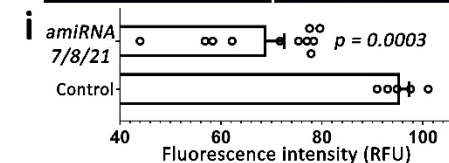
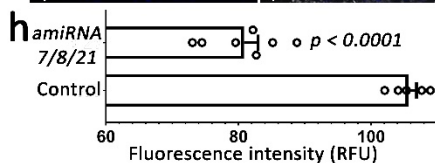
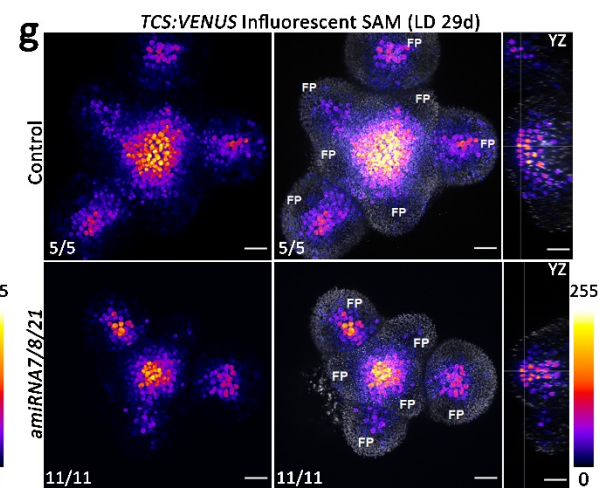
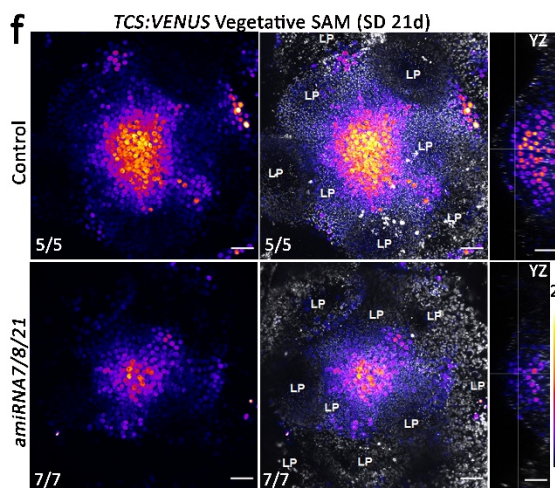
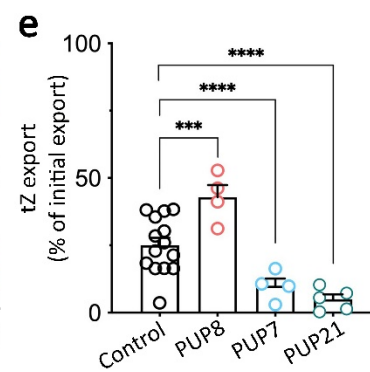
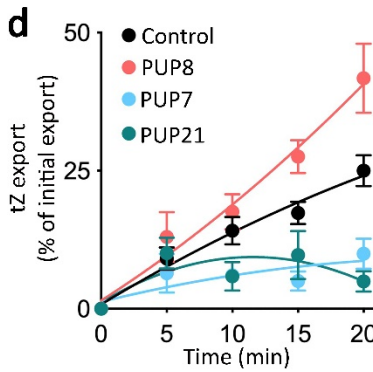
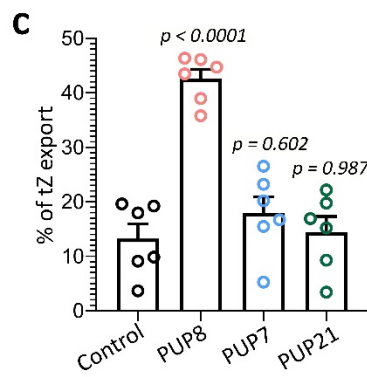
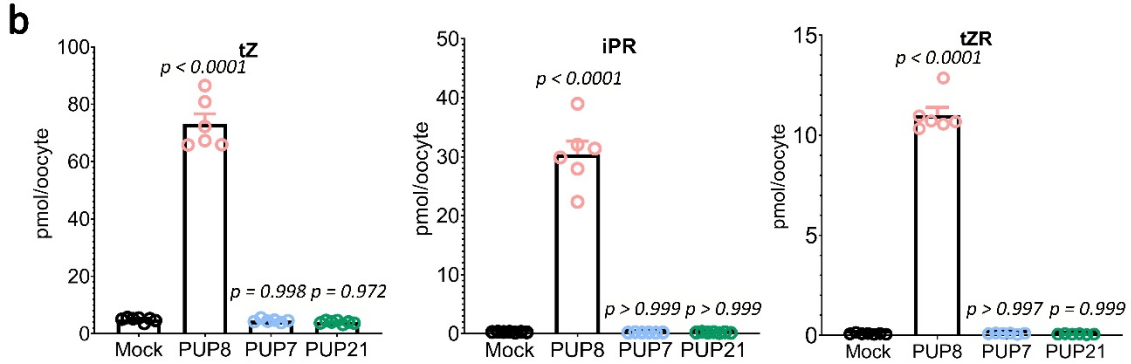
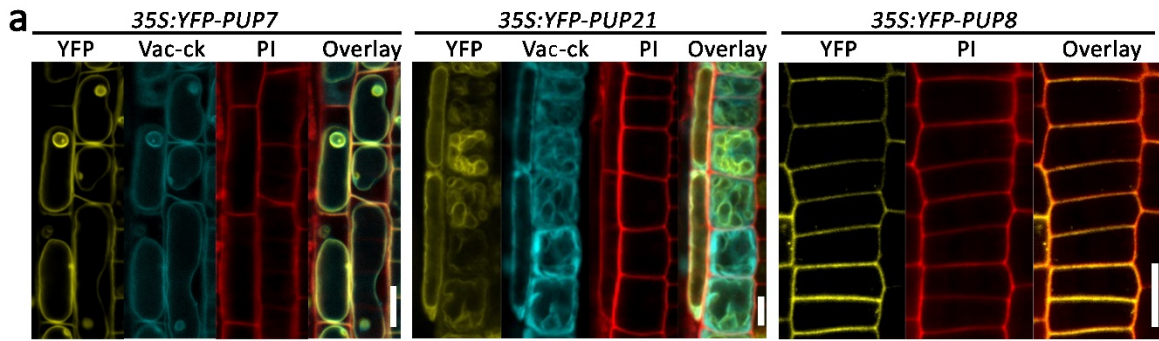
870

871

872

873

874



876 **Fig. 6: PUP7, PUP8, and PUP21 regulate cytokinin transport and shoot meristem.** **a**, Root meristem confocal
877 microscopy images of *35S:YFP-PUPs* localization. YFP (yellow) was used to label PUPs, Vac-ck (cyan) was used
878 as a tonoplast marker, and propidium iodide (PI) (red) was used to stain the cell wall. Scale bars = 10 μ m. **b**,
879 Standard import *Xenopus laevis* oocytes assays using the indicated cytokinin froms. 60 min transport assay
880 in 100 μ M cytokinins at pH = 5.5. n = 6-7, shown are means (\pm SE). *p* value two tailed *t* test is indicated for
881 each analysis. **c**, Injection-based export assay of PUPs in *Xenopus laevis* oocytes. n = 6 \pm SE, *p* value two-tailed
882 *t*-test is indicated for each analysis. **d, e**, tZ export from tobacco protoplasts as percentage of initial export as a
883 function of time (**d**) and at 20 minutes (**e**). n \geq 4, *** *p* < 0.001, **** *p* < 0.0001; One-way ANOVA. **f-i**,
884 *TCS-Venus* intensity in control plants (*TCS:VENUS*) compared to *amiR7/8/21* at (**f**) vegetative and (**g**)
885 inflorescence stages. *amiRNA7/8/21* stands for amiRNA triple knockdown *PUP7/8/21*. Optical longitudinal
886 sections of the meristem (YZ direction) are shown. Scale bars = 100 μ m. The color scale at the right indicates *TCS*
887 expression. Quantification of *TCS-Venus* intensity in vegetative (**h**) and inflorescence (**i**) stages. Control: n = 5 in
888 (**h, i**); *amiRNA7/8/21*: n = 7 in (**h**), n = 11 in (**i**). Shown are means (\pm SE). *p* value two tailed *t* test is indicated for
889 each analysis.
890

Supplemental Data

Multi-Knock – a multi-targeted genome-scale CRISPR toolbox to overcome functional redundancy in plants

Yangjie Hu¹, Priyanka Patra^{1,2,*}, Odelia Pisanty^{1,*}, Anat Shafir¹, Zeinu Mussa Belew³, Jenia Binenbaum¹, Shir Ben Yaakov¹, Bihai Shi², Laurence Charrier⁴, Gal Hyams¹, Yuqin Zhang¹, Maor Trabolsky¹, Omer Caldararu¹, Daniela Weiss¹, Christoph Crocoll³, Adi Avni¹, Teva Vernoux², Markus Geisler⁴, Hussam Hassan Nour-Eldin³, Itay Mayrose^{1,✉}, and Eilon Shani^{1,✉}

¹ School of Plant Sciences and Food Security, Tel Aviv University, Tel Aviv, 69978, Israel

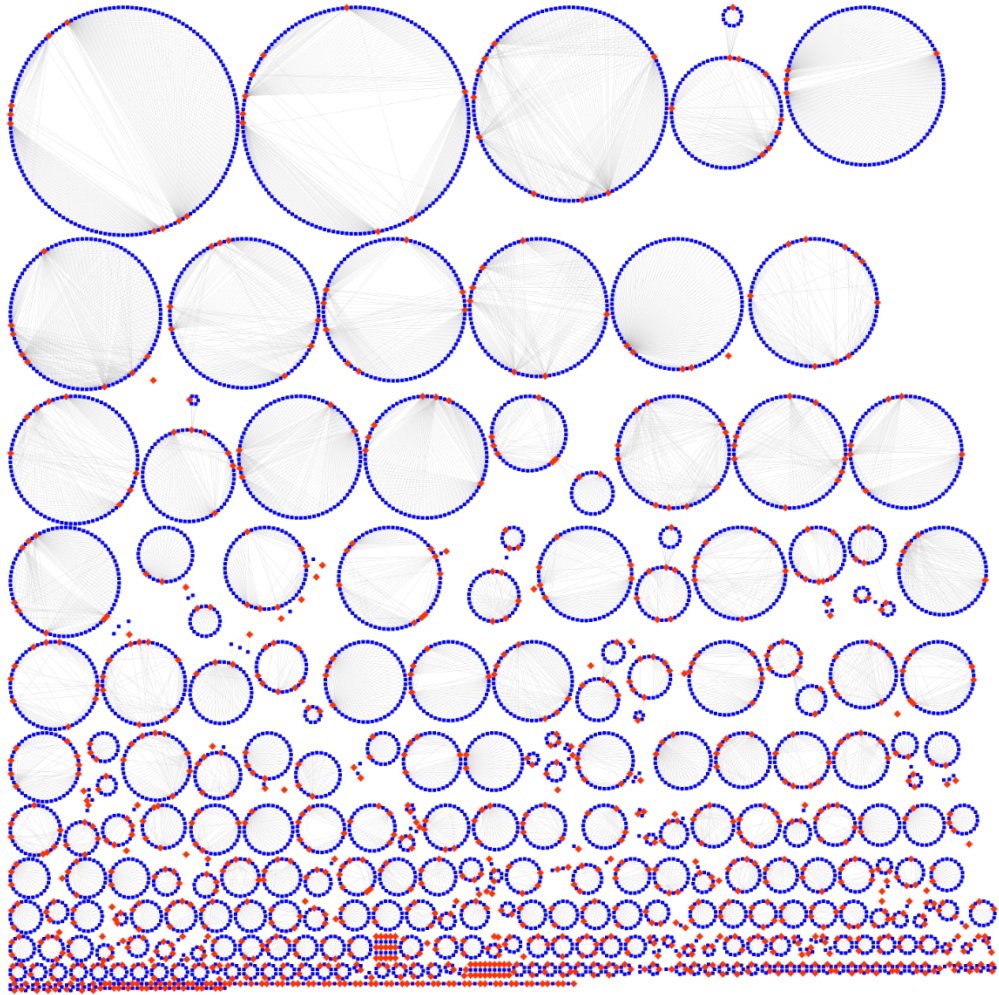
² Laboratoire Reproduction et Développement des Plantes, Université de Lyon, ENS de Lyon, UCB Lyon 1, CNRS, INRAE, INRIA, Lyon, France

³ DynaMo Center, Department of Plant and Environmental Sciences, University of Copenhagen, Frederiksberg, 1871, Denmark

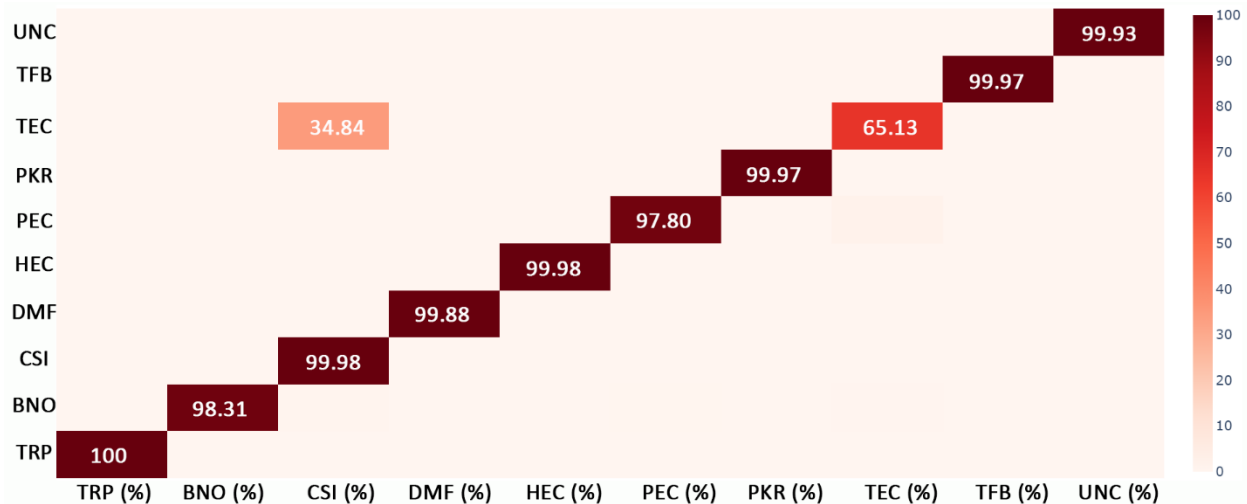
⁴ Department of Biology, University of Fribourg, CH-1700 Fribourg, Switzerland

* Equal contribution

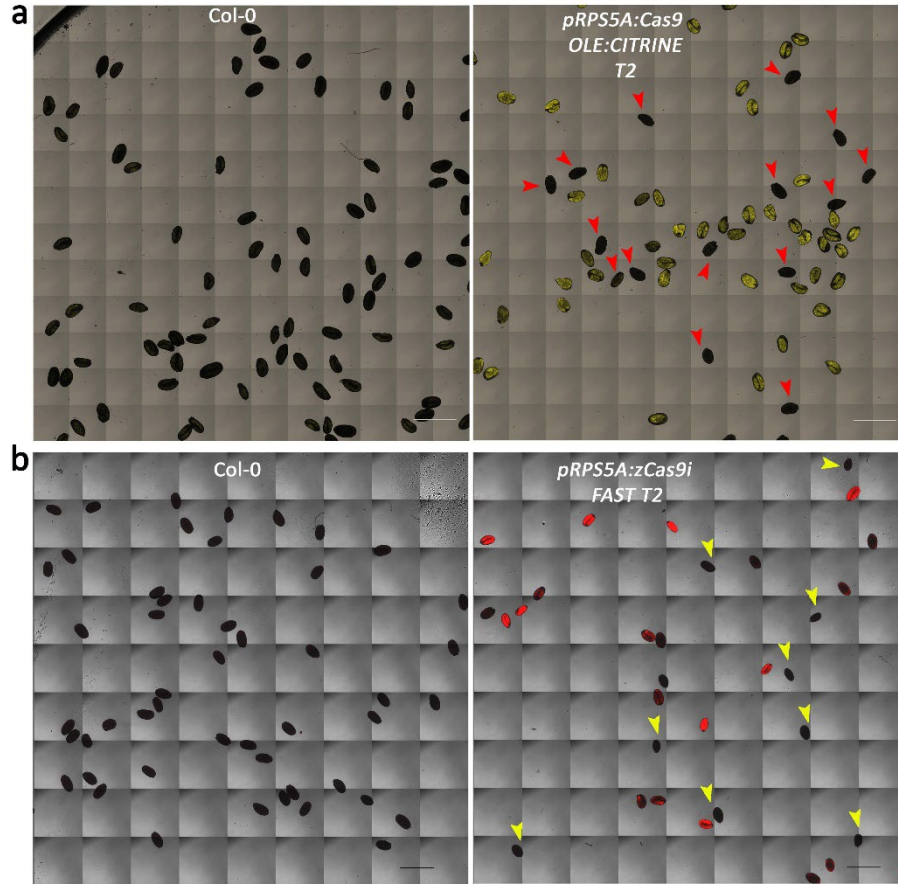
✉ Corresponding author



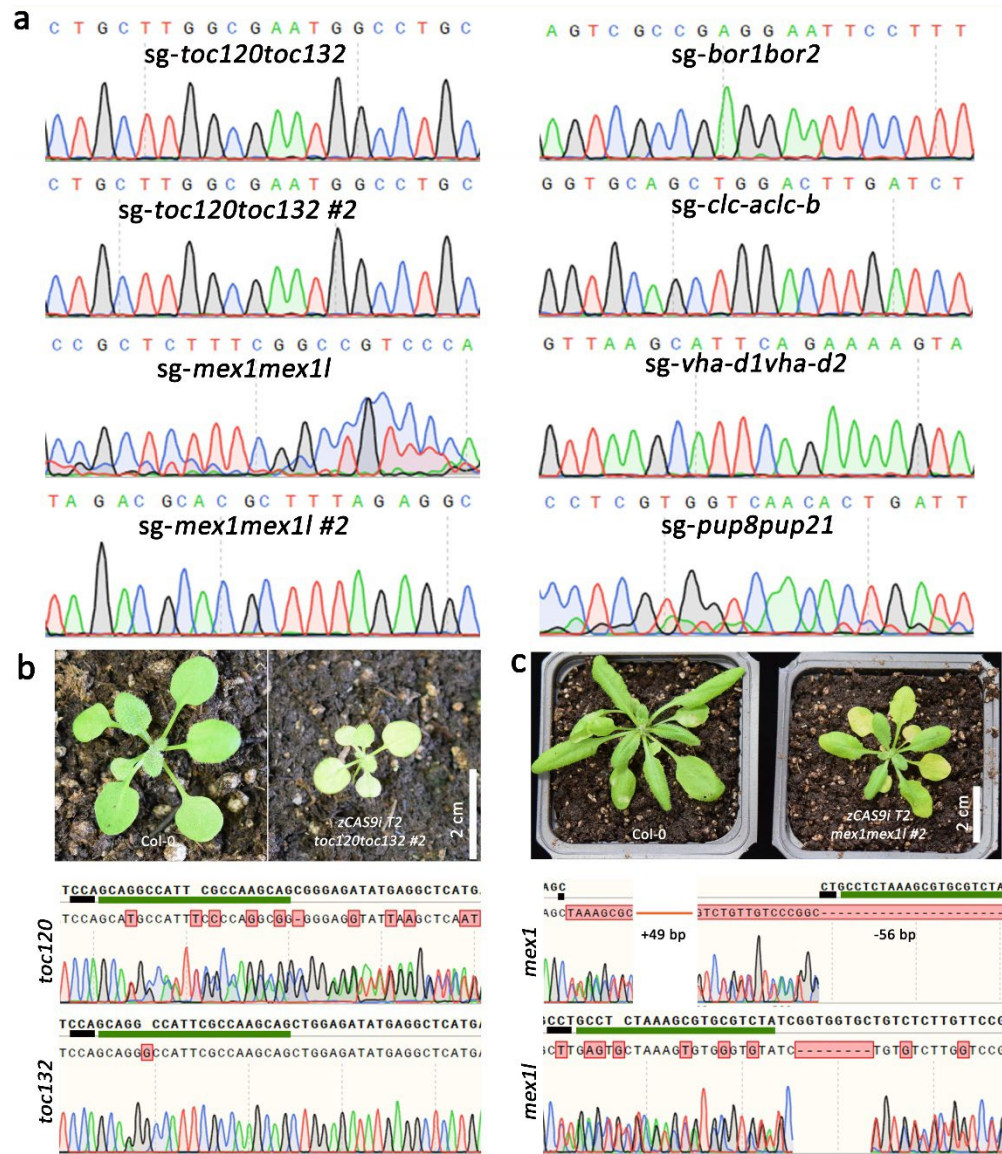
Supplementary Figure 1: Transportome Multi-Knock network. Overview of sgRNAs (blue) and the targeted genes (red) network for the CRISPR library targeting the transporters family. Shown are 1,123 transporter genes (red) and 5,635 sgRNAs (blue).



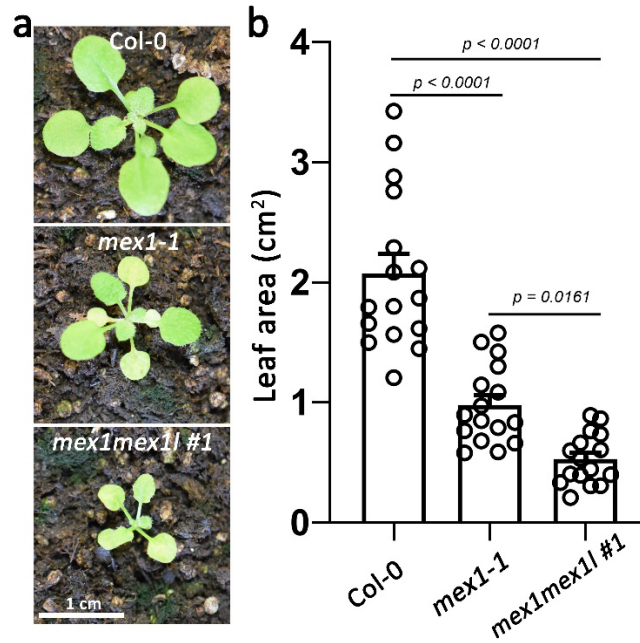
Supplementary Figure 2: sgRNAs cross-contamination analysis of the ten sub-libraries based on next-generation sequencing. Heatmap illustrating the percentage of sgRNAs for each individual sub-library. The color scale bar reflects the relative percentage. All libraries are highly specific, except for TEC which shows significant amplification of the CSI sub-library. TRP (transporters); PKR (protein kinases, protein phosphatases, receptors, and their ligands); TFB (transcription factors and other RNA and DNA binding proteins); BNO (proteins binding small molecules); CSI (proteins that form or interact with protein complexes including stabilizing factors); HEC (hydrolytic enzymes); TEC (metabolic enzymes and enzymes that catalyze transfer reactions); PEC (catalytically active proteins, mainly enzymes); DMF (proteins with diverse functional annotations not found in the other categories); and UNC (proteins of unknown function or cannot be inferred).



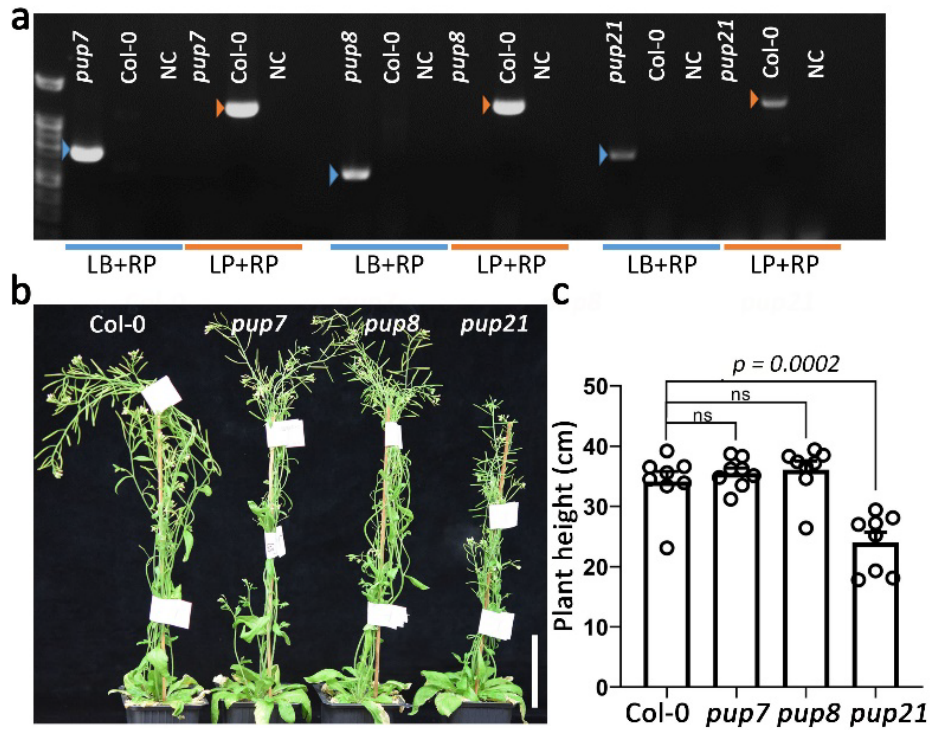
Supplementary Figure 3. Visual fluorescence segregation for Cas9-free seeds. **a**, Cas9-free seeds selection in pRPS5A:Cas9 OLE:CITRINE T2 seeds. Yellow signal in seeds indicates for OLE:CITRINE. The Cas9-free seeds, which do not produce the yellow fluorescence, are marked by red arrows. Scale bar = 1 mm. **b**, Cas9-free seeds selection in pRPS5A:zCas9i *FAST* T2 seeds. The Cas9-free seeds, which do not produce the red fluorescence, are marked by yellow arrows. *FAST* (pOLE1:tagRFP)¹. Scale bar = 1 mm.



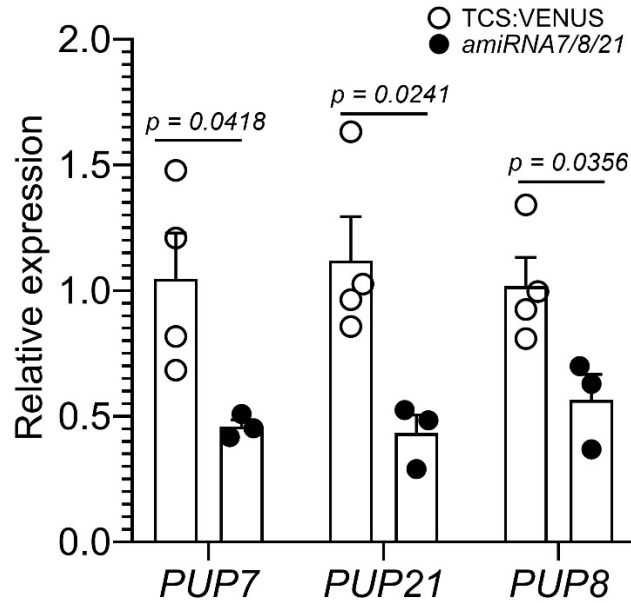
Supplementary Figure 4. Sequencing data for multiple sgRNA and their putative target genes. a, Chromatograms show sgRNA sequences of the indicated TRP Multi-Knock lines. Lines are presented in Fig 4. Two additional lines are presented for *toc132toc120* and *mex1mex1l* (#2). **b,c,** Shown are *toc132toc120* (**b**) and *mex1mex1l* (**c**) knockout alleles, which are additional to the lines presented in Fig 4. Photographs show an independent line for *toc120toc132* #2 (left). Chromatograms indicate for the types of mutation (left). Images show a similar independent line for *mex1mex1l* #2 (right). Chromatograms indicate for the types of mutation (right). Scale bar = 2 cm; PAM is marked with a black underline; 20-bp gRNA is underlined in green.



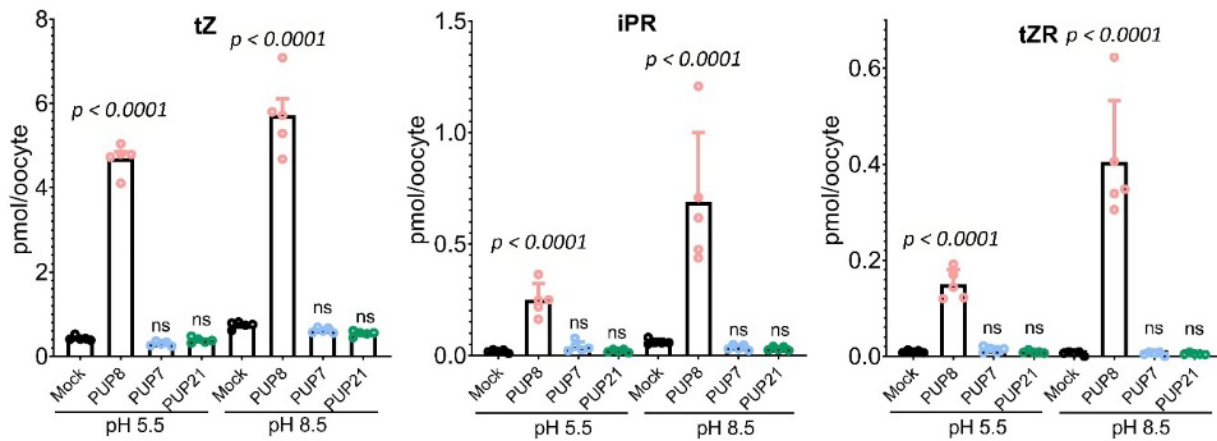
Supplementary Figure 5. *mex1* and *mex11*, single and double knockout phenotypes. a, Representative images showing shoot phenotypes of 18-day-old of the wild type (Col-0), single (*mex1-1*) and double mutant homozygous plants (*mex1mex11 T3 #1*). Scale bar = 1 cm. **b**, Quantification of phenotypes shown in (a). Shown are means (\pm SE), $n = 16$ plants, p value two tailed t -test is indicated.



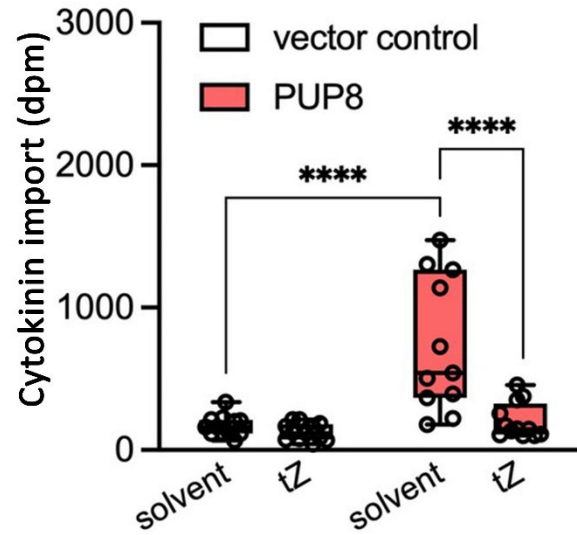
Supplementary Figure 7: Characterization of single T-DNA insertion mutants. **a**, Genotyping of the *pup7*, *pup8*, *pup21* single mutant plants compared to Col-0. Orange arrows indicate for WT amplification bands, blue arrows indicated for T-DNA insertion amplification bands. LB: left border primer of T-DNA insertion, LP: left genomic primer, RP: right genomic primer, NC: negative control. **b**, Plant height of 58-day-old plants of the indicated genotypes. **c**, Quantification of plant height. Shown are means (\pm SE), $n = 8$ plants, p value two tailed t -test is indicated. Scale bar = 5 cm



Supplementary Figure 8: PUP7, PUP8, and PUP21 are down-regulated in *amiR7/8/21*. Relative expression of the indicated PUP *amiR7/8/21*-targeted genes in 15-day-old seedlings, quantified by qRT-PCR. *amiRNA7/8/21* stands for amiRNA triple knockdown PUP7/8/21. Shown are averages (\pm SE), $n = 4$ (Control), $n = 3$ (*amiR7/8/21*); p value two tailed t test is indicated for each analysis.



Supplementary Figure 9: PUP8 promotes cytokinin uptake in *Xenopus laevis* oocytes. 60 min transport assay in 10 μ M cytokinin at pH = 5.5 and pH = 8.5. $n = 5 \pm$ SE, p value two tailed t -test is indicated for each analysis.



Supplementary Figure 10: PUP8 tZ competition assays. ^3H -tZ import into microsomal fractions prepared from tobacco leaves infiltrated with vector control and 35S:YFP-PUP8 (PUP8), conducted in the absence (solvent) and presence of a 1,000-fold excess of non-labelled tZ. Significant differences of means to solvent control were determined by ordinary One-way ANOVA; *** $p < 0.001$, **** $p < 0.0001$ ($n \geq 4$).

Supplementary Table 1. Overview of sgRNAs and gene numbers per family.

Families	Targeted genes per family (Coverage %)	Genes per family	sgRNAs per family
BNO	1443 (76.1%)	1896	5899
CSI	1399 (82.7%)	1692	4919
DMF	1343 (71.0%)	1891	5000
HEC	1438 (84.3%)	1706	6215
PEC	1252 (82.6%)	1515	4975
PKR	1190 (84.7%)	1405	6161
TEC	1041 (86.0%)	1211	4145
TFB	2042 (78.2%)	2611	6010
TRP	1123 (84.6%)	1327	5635
UNC	3881 (59.3%)	6544	10170

Supplementary Table 3. Primers for amplification of subgroups of sgRNA library

Pools	Forward primer (5'-3')	Reverse primer (5'-3')
PKR	CTGGTCATCATCCTGCCTTT	TTTGCCCCCTCCATATAACA
BNO	GGATTATTCATACCGTCCCA	CAAATGTGGTATGGCTGATT
CSI	AGAGCTCGTTTAGTGAACCG	GTGGTTTGTCCAAACTCATC
TFB	CGTTGGCTACCCGTGATATT	GCCCAGTCATAGCCGAATAG
TEC	TGTAAAACGACGGCCAGT	AACAGCTATGACCATGATTACG
PEC	GGAAACAGCTATGACCATG	GGTTTTCCAGTCACGAC
UNC	CGACTCACTATAGGGAGAGCGGC	AAGAACATCGATTTTCCATGGCAG
DMF	TCCTCCGCTTATTGATATGC	GGAAGTAAAAGTCGTAACAAGG
HEC	GCGAGAGTAGGGAAGTGC	AACATCAGAGATTTTGAGACAC
TRP	CCAAGCTATTTAGGTGACACGG	CCTCGACTGTGCCTTCTAGG

Supplementary Table 4. Primers for NGS PCR amplification and sgRNAs genotyping in transgenic plants.

Cas9 expression constructs	Forward primer (5'-3')	Reverse primer (5'-3')
pRPS5A:zCas9i	TACTAGATCGACGCTACTAG	CCGACTCGGTGCCACTTTT
pUBI:Cas9	CCCCTGGGAATCTGAAAGAAG	CCGACTCGGTGCCACTTTT
pEC:Cas9	CCCCTGGGAATCTGAAAGAAG	CCGACTCGGTGCCACTTTT
pRPS5A:Cas9 OLE:CITRIN	CCCCTGGGAATCTGAAAGAAG	CCGACTCGGTGCCACTTTT

Supplementary Table 5. Primers used for PCR-based genotyping.

Targets	Forward primer (5'-3')	Reverse primer (5'-3')
TOC120	CTCTTACGCACCATCACTG	GCTTCGGCAAGAATCTTGG
TOC132	TCTCCTGCGCACCATAAGT	TCACCATACTGCTGTTTCCAG
MEX1	AGGGAAATCCAGGTTTGGG	CTGCCACAGCAATACCAAAG
MEX1L	AGGGAAATCCAGGTTTGGG	GAGTAGAGACCACTCCAG
BOR1	GCTTTTCATGCAGCAAGCCA	GAACATCAAGCATCTCCTGC
BOR2	GGCCTTCTTATAGCTATGCTC	GGAAGTTGAAGCATCTCCTGA
CLC-a	GACACTCCCAATATGTTTGG	CAGAGGCAGATCCACATGT
CLC-b	GGAATCCCTGAGATCAAAGC	AGTACACCTCCAACAGGTG
VHA-d1	CCGCATCAACCTTTTCCATC	GAGGGTGTTCCTCATAATCTC
VHA-d2	CCCTTAGCTGTTTCATAACCC	CAAGGTATGCTTTGTAGAGGG
PUP7	CTCTTTTGCCAGCCACTAGCT	CCACAAGAAGAGCAGAGGATACAG
PUP8	CCCAAACCAAAAATCCCAAACC	CCAGGGATAGCAGCAATCCAA
PUP21	TTTCAGTACCTCAAACGAAGAACTGT	AGTACCACACAAGTTGCAACTAG
VPS53	GCTTGTGGCCCAAGTACATC	GGTAGCCTAGCGTTAAATTTG
VPS53-P	GATGTTGCTGGTTAGCCTCTT	GGGAGAGTAATCTGCTAGGTAG
SULTR4.1	GAAGTACTCCTGCTCTTGG	AGACGCAACATGACACAAC
SULTR4.2	GGCTTCAACCAATATACGG	CGAATAAGCCATCCAAGCC
SRP54	TACTGAGTTGTGATTCTTGC	AATGCTAAATCAATGCCATGA
SRP54-1	GCTGACAGGAAAAATGCTAAT	CTCATCCATATGCTCTCCTGTTC
PHT1.1	CTCTAGGAAATGGCCGAA	CCATTTAGTTGGATCTTAAACC
PHT1.2	GAGAGGCTTAGATGGCTGA	CCATTTAGTTGGATCTTAAACC
PHT1.3	GCGTACGATCTCTTTTGTGT	CATTAGTTGGATCGCAAACC

Supplementary Table 6. Genotyping primers for T-DNA lines

Gene	T-DNA Line	Primer name	Primer sequence (5'-3')
PUP7	SALK_084103	LP	TAAAGACACCCTCCATGTTCC
		RP	GAGAACTACACAACCTCGCAAC
		LB	ATTTTGCCGATTTTCGGAAC
PUP8	SALK_137526	LP	TCGTTGTTGACTTCCAAATCC
		RP	TGAGGATCAGTTGTACCAGGG
		LB	ATTTTGCCGATTTTCGGAAC
PUP21	GK-288E11	LP	AGCAAAAGGTACCTGATGACG
		RP	CTTTTCGTTCGAGGTAGTGCTG
		LB	ATAATAACGCTGCGGACATCTACATT

Supplementary Table 7. PUP cloning

Cloning primers. Gene	Forward primer (5'-3')	Reverse primer (5'-3')
<i>PUP7</i> genomic	caccATGGACAGATCTCAAGAACACTA TGCC	TCACACACTTTGTATGTTTGTGTGAC C
<i>PUP8</i> CDS	caccATGGAAATAACTCAAGTAATCTA TGT	TCATACACTATGTATGTTTGTGTGAC CTTCC
<i>PUP21</i> CDS	caccATGGGCATATCTCAAGTACACTA TTGC	TCATAAAGTTTGTGTTTCTTCCTCAA CAGGTT

Supplementary Table 8. MRM transitions for LC-MS/MS analysis.

Analyte	Retention Time [min]	Q1 [m/z]	Q3 [m/z]	CE [eV]	Reference
tZ [M+H] ⁺	1.25	220.0	136.0 ^{Qt}	15	(Ionescu et al. 2017)
tZR [M+H] ⁺	1.40	352.0	220.0 ^{Qt}	15	(Ionescu et al. 2017)
iPR [M+H] ⁺	1.60	336.1	204.0 ^{Qt}	15	(Ionescu et al. 2017)
		336.1	136.0	27	
		336.1	148.0	23	

Qt = quantifier ion, additional transitions were used for identification only; CE=collision energy; Q=quadrupole.

References:

1. Shimada, T. L., Shimada, T. & Hara-Nishimura, I. A rapid and non-destructive screenable marker, FAST, for identifying transformed seeds of *Arabidopsis thaliana*: TECHNICAL ADVANCE. *Plant J.* **61**, 519–528 (2010).